

THE EFFECTS OF ANTHROPOGENIC WARMING ON CHANGES OF EXTREME  
PRECIPITATION OVER KANSAS CITY METROPOLITAN AREA

A THESIS IN  
Environmental and Urban Geosciences

Presented to the Faculty of the University of  
Missouri-Kansas City in partial fulfillment of  
the requirements for the degree

MASTER OF SCIENCE

by  
KEVIN KANDOLA

B.S., University of Missouri-Kansas City, 2017 & 2019

Kansas City, Missouri  
2021

© 2021

KEVIN WALTER KANDOLA

ALL RIGHTS RESERVED

THE EFFECTS OF ANTHROPOGENIC WARMING ON CHANGES OF EXTREME  
PRECIPITATION OVER KANSAS CITY METROPOLITAN AREA

Kevin W. Kandola, Candidate for the Master of Science Degree  
University of Missouri-Kansas City, 2021

ABSTRACT

When the Intergovernmental Panel on Climate Change (IPCC) *Special Report Global Warming of 1.5°C* was released in 2018 it postulated about the devastating effects of a 2° C increase in global temperature, based on projections of coarse resolution global climate models (GCMs). While GCMs are useful tools to examine global- and continental-scale climate change, policy makers are more interested in climate change from regional and local perspectives. In order for municipalities to accurately prepare for the climate change impacts on their infrastructure, higher-resolution climate models are needed. This research developed a high-resolution (1-kilometer) dynamical climate downscaling framework using the Weather Research and Forecasting (WRF) regional climate model and applied it to the Kansas City metropolitan area. Two initial simulations are first performed to reproduce a devastating storm in March 2019 known as winter storm Ulmer, which flooded major portions of the Midwest's farmlands causing an estimated \$3 billion dollars in damage. These initial simulations used different landcover inputs to represent present-day, i.e., control, and historic land use as the other initial simulation. Then a suite of sensitivity experiments was designed and performed for both initial simulations to investigate potential changes to the region's precipitation under various global warming and cooling scenarios.

## APPROVAL PAGE

The faculty listed below, appointed by the Dean of the College of Arts and Sciences have examined a thesis titled “The Effects of Anthropogenic Warming on Extreme Precipitation Events Over Kansas City Metropolitan Area,” presented by Kevin W. Kandola, candidate for the Master of Science degree, and certify that, in their opinion, it is worthy of acceptance.

### Supervisory Committee

Fengpeng Sun, Ph.D., Committee Chair  
Department of Earth and Environmental Sciences

Wei Ji, Ph.D.  
Department of Earth and Environmental Sciences

Jejung Lee, Ph.D.  
Department of Earth and Environmental Sciences

Jimmy Adegoke, Ph.D.  
Department of Earth and Environmental Sciences

# CONTENTS

ABSTRACT .....	iii
LIST OF ILLUSTRATIONS.....	vii
LIST OF TABLES.....	ix
ACKNOWLEDGEMENTS.....	x
Chapter	
1. INTRODUCTION .....	1
1.1 Project Introduction .....	1
1.2 Extreme Weather History .....	2
1.2.1 Extreme Precipitation Damage Assessment .....	2
1.2.2 Winter Storm Ulmer .....	2
1.3 IPCC Predictions.....	5
1.4 Clausius-Clapeyron Equation .....	7
2. Global Climate Models and Downscaling .....	9
2.1 CMIP 5 Predictions.....	9
2.2 Statistical and Dynamical Downscaling .....	18
2.3 Benefits of Regional Climate Models.....	19
3. Methodology .....	21
3.1 Area-of-Interest.....	21
3.2 WRF and Parameters .....	21
3.3 Model Setup.....	23
3.3.1 Initial Data .....	23
3.3.2 Domains.....	23

3.3.3 Land Cover for 2016 Simulation .....	26
3.3.4 Land Cover for 1938 Simulation .....	27
3.3.5 Observational Analysis .....	29
3.3.6 Sensitivity Experiments .....	30
3.3.7 Experimental Design.....	31
4.RESULTS .....	33
4.1 Observational Analysis of 2016 Control .....	33
4.1.2 Analysis of the Initial Simulations.....	39
4.2 Sensitivity Simulation Results .....	42
4.2.1 Precipitation Results for 2016.....	42
4.2.2 Precipitation Results for 1938.....	44
4.2.3 Temperature Analysis for 2016 .....	47
4.2.4 Temperature Analysis for 1938 .....	49
4.3 Joint Analysis.....	51
4.3.1 Precipitation Analysis Between 1938 and 2016 Simulations .....	51
4.3.2 Temperature Analysis .....	54
5.DISCUSSION AND CONCLUSIONS .....	56
5.1 Control Simulation Evaluation .....	56
5.2 Sensitivity Simulation Analysis.....	57
5.3 Joint Analysis.....	58
5.4 Conclusion .....	59
REFERENCES .....	61
VITA.....	67

## ILLUSTRATIONS

Figure	Page
1. Offutt Airforce Base Flooding .....	4
2. Offutt Airforce Base Flooding From Satellite .....	5
3. CMIP 5 Decadal Simulations Using RCP 8.5 .....	7
4. RCP Table .....	12
5. Annual Mean Temperature and Precipitation Predictions .....	14
6. Summer Mean Temperature and Precipitation Predictions .....	15
7. Fall Mean Temperature and Precipitation Predictions.....	16
8. Winter Mean Temperature and Precipitation Predictions.....	17
9. Spring Mean Temperature and Precipitation Predictions .....	18
10. Domain 1 Topographical Map 9km.....	24
11. Domain 2 Topographical Map 3km.....	25
12. Domain 3 Topographical Map 1km.....	26
13. Domain 3 NLCD 2016 Land Use .....	27
14. Domain 3 1938 Land Use .....	29
15. Weather Station Locations .....	30
16. Lee’s Summit Airport Precipitation.....	34
17. Downtown Airport Precipitation.....	35
18. New Century Aircenter Airport Precipitation.....	36
19. Olathe Airport Precipitation.....	37
20. MCI Airport Precipitation.....	38

21. Pixel-to-pixel Difference Between 1938 and 2016 Initial Simulations Domain 2 is Represented by A Domain 3 is Represented by B.....	40
22. Domain 3 Difference in Temperature From Initial Simulations of 1938 and 2016...	42
23. Difference in Temperature From 2016 Sensitivity Simulations Compared to Initial Simulation Domain 3 .....	44
24. Difference in Precipitation From 2016 Sensitivity Simulations Compared to Initial Simulation Domain 2 .....	45
25. Difference in Precipitation From 1938 Sensitivity Simulations Compared to Initial Simulation Domain 3 .....	47
26. Difference in Precipitation From 1938 Sensitivity Simulations Compared to Initial Simulation Domain 2 .....	48
27. Difference in Averaged T2 From 2016 Sensitivity Simulations Compared to Initial Simulation Domain 3 .....	50
28. Difference in Averaged T2 From 1938 Sensitivity Simulations Compared to Initial Simulation Domain 3 .....	51
29. Difference in Precipitation From 1938 and 2016 Sensitivity Simulations for Domain 2 .....	55
30. Difference in Precipitation From 1938 and 2016 Sensitivity Simulations for Domain 3 .....	56
31. Difference in Average T2 from 1938 and 2016 Sensitivity Simulations for Domain 3 .....	58

## TABLES

Table	Page
1. Parameters Used in All Simulations For This Study .....	22
2. Observed vs Present-day Simulation Weather Station Totals .....	38
3. Precipitation Percent Change and Average Change between Initial 1938 and 2016 Simulations .....	41
4. T2 Percent change and Mean Change between Initial 1938 and 2016 Simulations..	42
5. Precipitation Difference Between 2016 Initial Simulation and Sensitivity Simulations .....	43
6. Precipitation Difference Between 1938 Initial Simulation and Sensitivity Simulations .....	46
7. T2 Average Difference and Absolute Max Difference for 2016 .....	51
8. T2 Average Difference and Absolute Max Difference for 1938 .....	53
9. Precipitation Average Percent Change Between Historic and Present-day Sensitivity Simulations .....	57
10. T2 Average Difference and Absolute Max Difference between Historic and Present- day Sensitivity Simulations.....	59

## ACKNOWLEDGEMENTS

I would like to thank Dr. Fengpeng Sun for supporting me through his Missouri Established Program to Stimulate Competitive Research (EPSCoR) funding both as an Undergrad and through my Graduate school. I would also like to thank Dr. Sun for helping guide me and motivating me through my time at the University of Missouri – Kansas City. I would also like to thank UMKC for providing me with the Summer Undergraduate Research Opportunity (SUROP) grant during my undergraduate in 2019. I would like to thank the Earth and Environmental Sciences department for the Newcomb Student Research Assistance funds in 2019 and for providing me with the NASA Missouri Space Grant Consortium Fellowship in 2020. I would like to also thank the School of Graduate Studies for providing me with their Travel Grant in 2021 to present my work at both American Meteorological Society (AMS) and American Geophysical Union (AGU) conferences.

Next, I would like to thank Dr. Ji, Dr. Adegoke, and Dr. Lee, for agreeing to be on my committee and providing feedback on my research. I would also like to thank them for being great teachers during my time at UMKC and for helping me learn more about my interests and finding new ones along the way. I would also like to thank Lili, and Jianfen from my lab for helping me work through problems during their time in our lab and Kyle for helping me with my research during my undergraduate and my graduate school. I would also like to thank my family for helping me to support me not just through my time at UMKC, but through my entire life and to my brother Tej for constantly pushing me out of my comfort zone and getting me to continue my schooling and never letting me give up.

## CHAPTER 1

### INTRODUCTION

#### 1.1 Project Introduction

In March of 2019 winter storm Ulmer tracked across the United States with estimates of over \$2.9 billion in damages. Extreme precipitation events like Ulmer have become more common with the increase being linked to anthropogenic warming. Winter storm Ulmer was a spring storm that underwent a process called bombogenesis, which occurs when there is an increase in instability in the atmosphere, allowing the storm to become much more powerful. By the end of February, prior to Ulmer, Nebraska had recorded 27 inches of snow, compared to the average 6 inches (NASA, 2019; Nebraska Department of Natural Resources, 2019). This above average snowfall caused areas around Nebraska to have as much as 16 inches of snow on the ground leading up to Ulmer (US Department of Commerce, 2019). When Ulmer came across the Midwest the land surrounding the Missouri River was still frozen or covered in snow from a previous storm, which caused the excessive precipitation of Ulmer to cause historic flooding across the area. This historic flooding caused levees to breach, roads to be washed away, and farmlands to be destroyed throughout the Midwest. This study is designed to first use a Regional Climate Model (RCM) to re-create Ulmer, then manually alter the temperature to study the effect of warming temperatures, that are expected with climate change, on precipitation events. In this study a present-day landcover will be used for one set of sensitivity simulations, where another set will be ran using historical landcover to study how urban sprawl may affect the precipitation events.

## 1.2 Extreme Weather History

### 1.2.1 Extreme Precipitation Damage Assessment

Between 1988 and 2017, it was estimated that the about one-third (\$73 billion) of the total cost of flood damage in the United States was a result of increases in precipitation events (Davenport, 2020). The flood damage caused by these changes were estimated to cost between \$39 to \$91 billion of the roughly \$200 billion in total damage. Between 1960 and 2009, nearly 85% of all natural hazards damage and losses could be attributed to severe atmospheric and hydrological events (Gall et al., 2011). The United States Army Corps of Engineers (USACE) expressed the need for repairs after the spring of 2019 flooding from extreme weather caused \$20 billion in damages (USACE, 2021). If the cost of damages from these storms continue to escalate as it has in the past two decades, then losses of up to \$400 billion per decade could become reality (Gall et al., 2011). In 2021 the USACE released their grade for the United States' levee systems, where they gave it an overall rating of "D". The United States levee system protects \$2.3 trillion in properties and consists of nearly 30,000 miles of levees and they estimate about \$21 billion in upgrades and repairs are needed to keep up with increasing flood threats (USACE, 2021).

### 1.2.2 Winter Storm Ulmer

The storm that will be used in this study is Winter Storm Ulmer that formed on March 8, 2019, and lasted until March 16. This storm was categorized as a "bomb cyclone" after undergoing bombogenesis which is defined as barometric pressure readings within the storm dropping more than 24mbar within a 24-hour period (Weather Channel, 2019; NOAA, 2021). This winter storm impacted a large portion of the country causing 100mph gusts of

wind in New Mexico (Weather Channel, 2019), severe flooding and failure of multiple levees following the Missouri River (Norvell, 2019). This storm caused devastating flooding across the Midwest with an estimated one million acres of farmland inundated with water that caused either crops to fail or the land to be unfarmable, costing billions of dollars to the agricultural economy (Huffstutter, 2019). In 2011, the Offutt Air Force Base in Nebraska came close to flooding, and the need to increase the height of the levee system around it was documented. They were also told that the levee would be de-certified in 2017 if actions were not taken (Irfan, 2019). In 2019, flood waters breached the levees around Offutt Air Force Base and reached up to nine feet deep in some areas, causing one-third of the base to flood and forcing jets to relocate to other bases Figures (1, 2).



Figure 1. Shows the flood waters covering parts of Offutt Air Force Base where up to 9 feet of flood waters destroyed buildings and forced planes to be relocated. Source: U.S. Air Force photo, by Tsgt. Rachelle Blake



Figure 2. Shows the Missouri river at its normal level with surrounding areas near Offutt Air Force Base on the left and on the right shows the Missouri river water level after winter storm Ulmer. Source: NASA Earth Observatory

### 1.3 IPCC predictions

In 2014, the International Panel on Climate Change (IPCC) released their Fifth Assessment Report (AR5), where they stated that surface temperatures are expected to increase throughout the 21<sup>st</sup> century under all emission scenarios, and it is very likely that temperature increases will cause extreme precipitation events to become more intense and frequent in many areas around the world (IPCC, 2014). In 2018, the IPCC released the Special Report on Global Warming of 1.5°C (SR15). This report was focused on the effects of global warming of 1.5°C above pre-industrial levels to help increase knowledge and better

prepare the world for what is predicted to come so that preparations can be made. The SR15 states that there is substantial evidence that anthropogenic warming has led to an increase in frequency, intensity, and amount of heavy precipitation events at the global scale (IPCC, 2018).

In 2008, groups of modelers from around the world came together to create the Coupled Model Intercomparison Project Phase 5 (CMIP5). The purpose of CMIP 5 was to help predict both near (out to about 2035) and long term (past 2100) climate change. In Figure 3, the global climate model results from the CMIP5 show an increase of precipitation across most of the United States with an exception being found in the Southwest portion where decreased precipitation is expected to occur. The top of Figure 3 shows an increase in mean temperature for the entire globe across the decadal run, which is agreed upon by at least two-thirds of the models within CMIP5. Over the United states the changes in precipitation are less agreed upon, but precipitation is expected to increase to some extent across the country with an exception found in the Southwest.

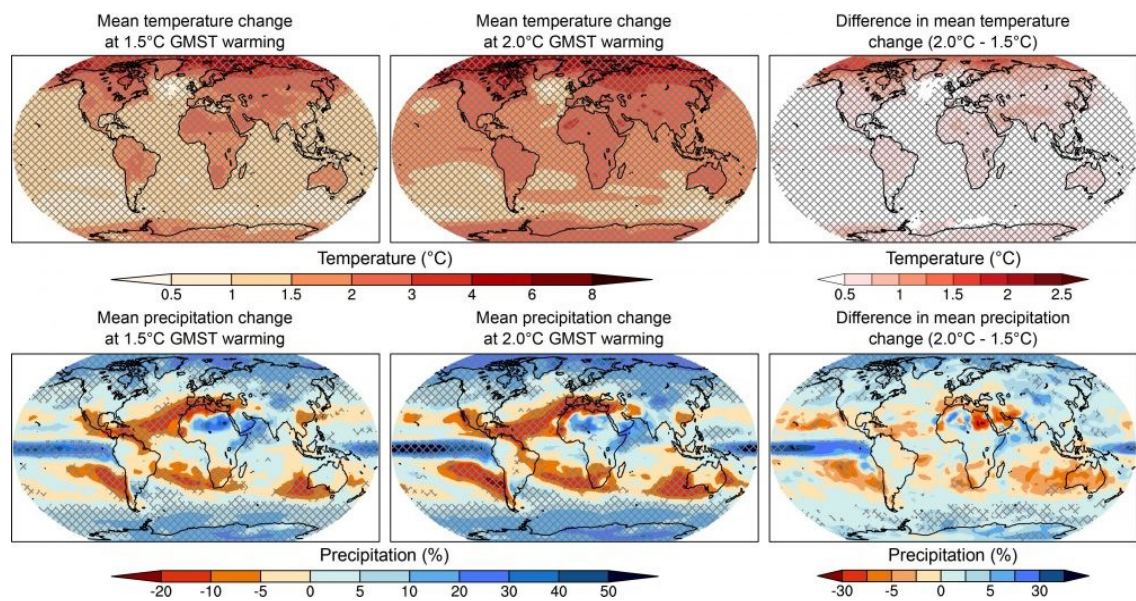


Figure 3. Shows results of CMIP 5 model simulations ran for 10 years at a given radiative forcing of RCP 8.5. The cross-hatching represents where at least two-thirds of the models agree. Source: (IPCC, 2018)

#### 1.4 Clausius-Clapeyron Equation

In this study the same precipitation event, i.e., winter storm Ulmer, will be simulated with its initial forcing data in addition to using a suite of sensitivity experiments by changing the temperature across domains. The purpose for these sensitivity experiments will be to see if precipitation results follow the Clausius-Clapeyron (C-C) equation. The C-C equation was developed by Rudolf Clausius and Benoît Paul Émile Clapeyron in the 1830s. The C-C equation in Equation 1 is defined by saturation vapor pressure ( $e_s$ ), temperature ( $T$ ), specific latent heat of evaporation of water ( $L_v$ ), and the gas constant of water vapor ( $R_v$ ).

$$\frac{de_s}{dT} = \frac{L_v(T)e_s}{R_v T^2}$$

Equation 1. Shows the C-C equation used in atmospheric research for measuring atmospheric moisture change compared to temperature change.

The Clausius-Clapeyron equation states that an increase of 1° Celsius increases the amount of moisture that can be held in the air by 7% (Barberok, 2016; Ali et al., 2018). This increase in atmospheric moisture is essential fuel needed to make these storms more intense (Tandon, 2018). The temperature increase that is associated with climate change causes an increase in the rate of evaporation of water from the Earth's surface. The increase in evaporation causes a rise in atmospheric moisture, contributing to more powerful storm

development and longer storm duration. The C-C equation assumes that the relative humidity remains constant through all temperature increases (Lenderink, 2017). The change in relative humidity gives an explanation as to why Missouri is expected to become drier during the summer and fall months in Figures 6 and 7. The increase in temperatures during the summer and fall months would cause the relative humidity to likely lower as this time is relatively dry to begin with and further temperature increases would cause this to become exacerbated.

Some studies have shown precipitation surpassing the C-C equations estimations. In higher latitudes it has been estimated that precipitation would be close to 6.5% per Kelvin, while at lower latitudes, near the equator, where precipitation events are driven more by latent heat released by other precipitation events, it is expected that the increases seen could be closer to 25% (Allen and Ingram, 2002). In an earlier study, Lenderink (2011) found that using the dewpoint temperatures prior to precipitation events consistently showed this super-CC value of 12-14% increase per degree Celsius. These findings showing this super-C-C relationship mean that these precipitation events could exceed expectations with the anticipated warming tied to anthropogenic warming.

The values that will be assessed in this study are the precipitation totals over each domain and the temperature at two meters (T2) for both the 2<sup>nd</sup> and 3<sup>rd</sup> domain. The goals for this study are first to see how the changing temperature values will affect the same precipitation event. The second portion is to look at how the changing land cover will affect the T2 and precipitation values during the event over the entire domain. This will be done by looking at the differences between the sensitivity experiment and their respective initial simulation and also the 2018 simulations compared to the 1938 simulations.

## CHAPTER 2

### GLOBAL CLIMATE MODELS AND DOWNSCALING

#### 2.1 CMIP 5 Predictions

The Environmental Protection Agency has created a user-friendly tool called the Locating and Selecting Scenarios Online (LASSO) to provide users with access to Coupled Model Intercomparison Project Phase 5 (CMIP 5) data. LASSO allows users to view climate change projections to help them answer their specific questions. The CMIP 5 data is created using thirty-five individual global climate models (GCMs) that have a much lower resolution (70-400km) than the regional climate models, like the one used in this study. The LASSO tool helps users to create scatterplot data to see their chosen projection data, which is shown in Figures 5, 6, 7, 8, and 9. The data downloaded for these figures were obtained from the LASSO tool so that only data over the state of Missouri would be included.

A key aspect of future climate scenarios is the Representative Concentration Pathway (RCP), which are different scenarios that assume different radiative forcing levels based on differing mitigation plans (Figure 4). These RCPs were developed through a collaboration of integrated assessment modelers, climate modelers, terrestrial ecosystem modelers, and emission inventory experts after the IPCC requested new emission scenarios to be developed for future climate change assessment (IPCC, 2017; van Vuuren et al., 2011). This collaboration within the modeling community provided four separate possible trajectories for greenhouse gas emissions through the year 2100 that would allow comparison between separate studies using the same dataset (van Vuuren et al., 2011). The four RCPs are 2.6, 4.5, 6.0, and 8.5, which show separate tracks of the predicted radiative forcing that could occur through the end of the century and were picked to cover the possible variations in radiative

forcing of 2.6 W/m<sup>2</sup>- 8.5 W/m<sup>2</sup> (Fisher et al. 2007; Van Vuuren and Riahi 2011). These four levels that were selected were based off forcing greenhouse gases and other forcing agents such as landcover change (van Vuuren et al., 2011). RCP 2.6 was labeled as a mitigation scenario because it leads to the lowest increases in radiative forcing. RCP4.5 and 6 were labeled as stabilization scenarios, and RCP8.5 was labeled as a business-as-usual scenario due to having no climate change interventions applied (van Vuuren et al., 2011).

LASSO data that is available in different statistically downscaled data sets, such as Bias Corrected Spatially Downscaled (BCSD), Localized Constructed Analogs (LOCA), and Multivariate Adaptive Constructed Analogs (MACA). These data sets are created using the coarse-resolution data from the CMIP5 GCMs, which are then downscaled to regional scale using various statistical techniques that look at meteorological observations to remove historical biases and try to match spatial patterns in the output (Abatzogluo and Brown, 2012; Pierce et al., 2015). The historical bias correction that is done to these data sets is then recorded and used for future projections. In Figure 5, the scatterplots show the expected annual precipitation and temperature change at the end of the century using the RCP4.5 and 8.5 scenario. The annual prediction for RCP8.5 in Figure 5b show a general agreement of an increase of over 5°F in the mean annual temperature, and a majority of the models show an increase in the mean annual precipitation in the state of Missouri. The RCP4.5 scenario shows a similar distribution as the RCP8.5 scenario, however the temperature and precipitation values are about half of what is found in the more extreme scenario.

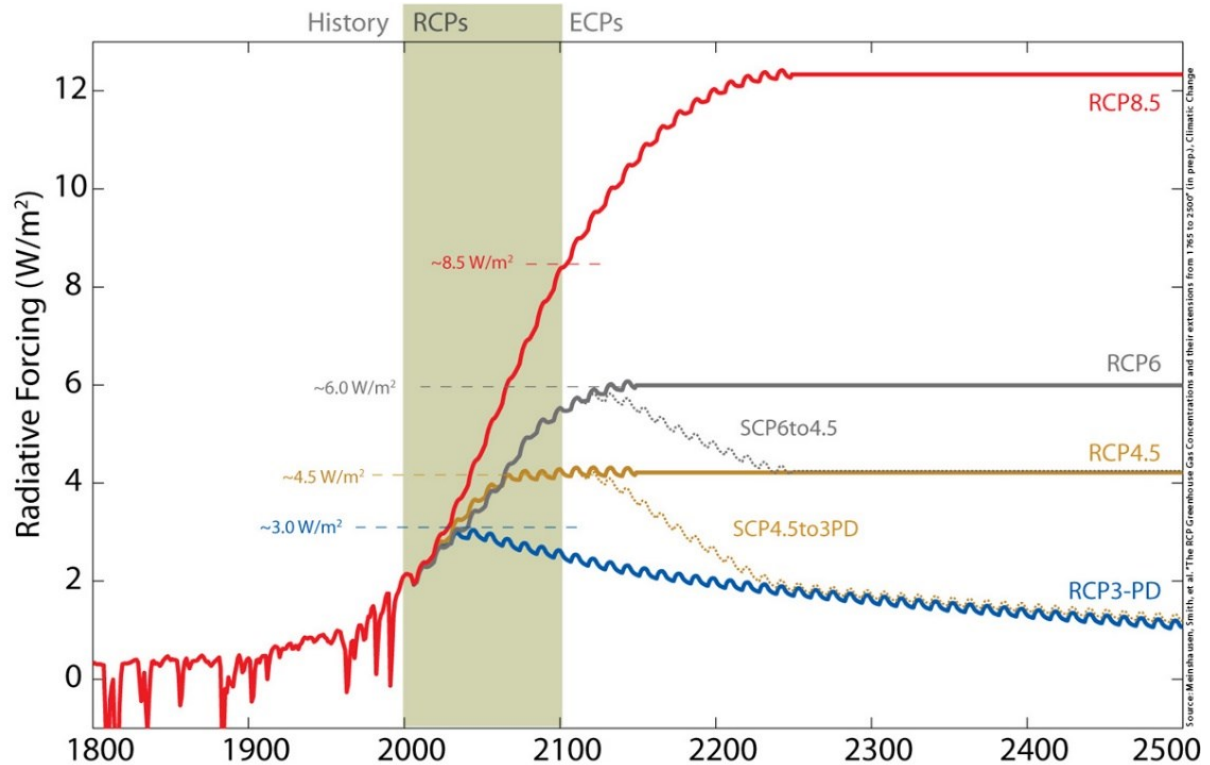


Figure 4. The expected radiative forcing for the different RCP scenarios with present day until the end of the 21<sup>st</sup> century highlighted. **Source:** Postdam Institute for Climate Impact Research

When the data is split into different seasons, a pattern for increased seasonal precipitation becomes more evident. In Figure 6a, the RCP4.5 scenario shows an increase in summer temperature of about 2.5°-9°F, and has more models showing an increase in precipitation than Figure 6b; however, there are drastic decreases of over 30% in precipitation. In Figure 6a there are anticipated decreases in precipitation in the summer months, however the increase in temperature across the sampled models ranges from 6°-16°F. In Figure 7a there is a much wider variation in temperature and precipitation between the models compared to the summer models shown in the Figure 6a. The precipitation for RCP 4.5 in the fall is a lot more undecided showing a range from -20 to +20% with the

models showing a fairly even distribution within that range. The Fall season in Figure 7b shows a similar increase in temperature to the summer results although there is a more variation on precipitation change. The winter season shown in Figure 8a shows a fairly agreed upon increase in precipitation between 5-20% for most models, with an increase in temperature from 2.5°-8°F. Figure 8b shows an increase in temperature from 4°-13°F with most models showing an increase in precipitation falling between 15-30% for the RCP 8.5 scenario. These seasonal scatterplots show more agreement on an increase or decrease in precipitation between models when compared to the annual mean precipitation.

The focus of this research is Winter storm Ulmer, which occurred in March 2019, so attention should be drawn to the spring months shown in Figure 9. In Figure 9a, there is an agreement between models that there will be an increase in precipitation of 5-20%. Figure 9a also shows an increase ranging from 2.5-7°F across all models for the RCP 4.5 scenario. The data shows that all but two models have some increase in precipitation for these months, and all but nine of those in agreement show an increase of over 10% precipitation in the spring. The data in Figure 9b also show an increase in temperature during the season in which winter storm Ulmer happened. Both temperature and precipitation will be looked at in this study to see if these results continue at the local resolution.

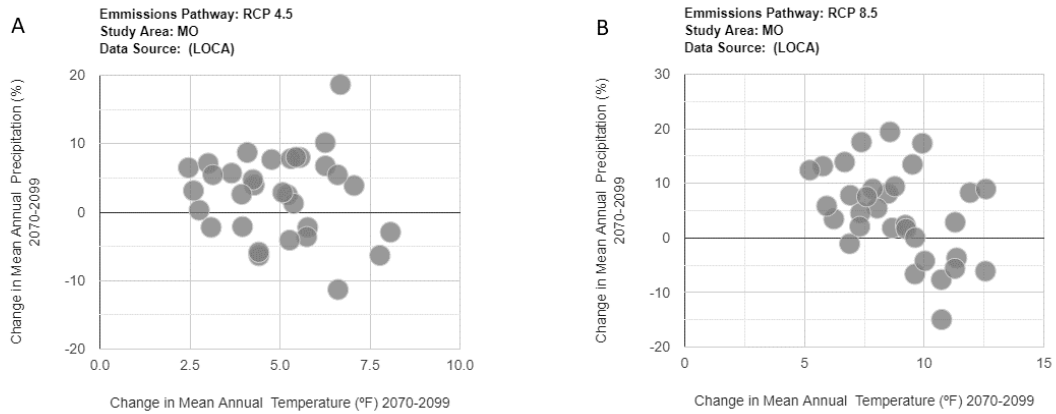


Figure 5. Shows the annual mean precipitation change along the Y axis and the mean annual temperature change along the X axis for each model used in CMIP 5. These models are representing the RCP 8.5 scenario at the end of the century. Source: EPA. EPA, Environmental Protection Agency, 2021, [lasso.epa.gov/strategies](https://www.lasso.epa.gov/strategies).

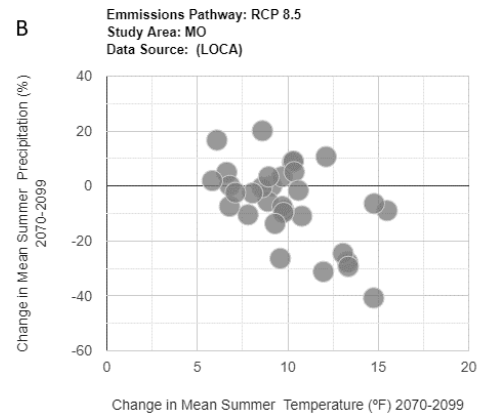
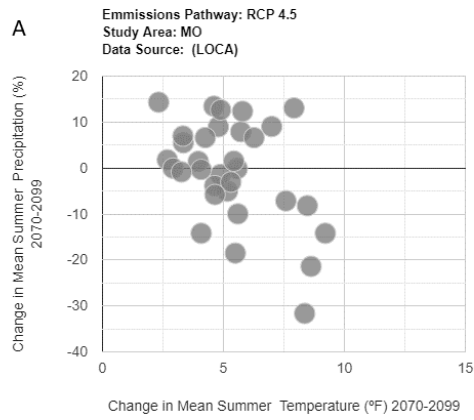


Figure 6. Same as Figure (5), but is for the summer (JJA). Source: EPA. EPA, Environmental Protection Agency, 2021, [lasso.epa.gov/strategies](https://www.lasso.epa.gov/strategies).

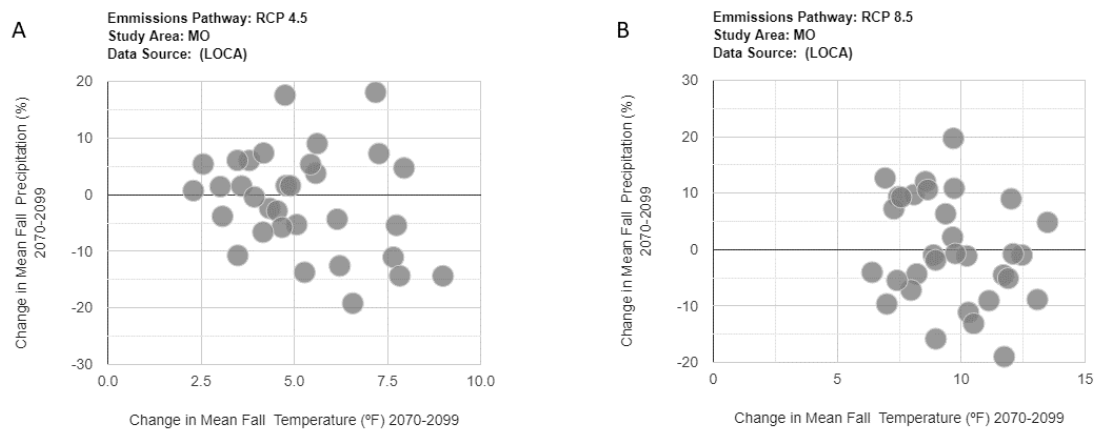


Figure 7. Same as figure (5), but is for the Fall (SON). Source: EPA. EPA, Environmental Protection Agency, 2021, [lasso.epa.gov/strategies](https://www.lasso.epa.gov/strategies).

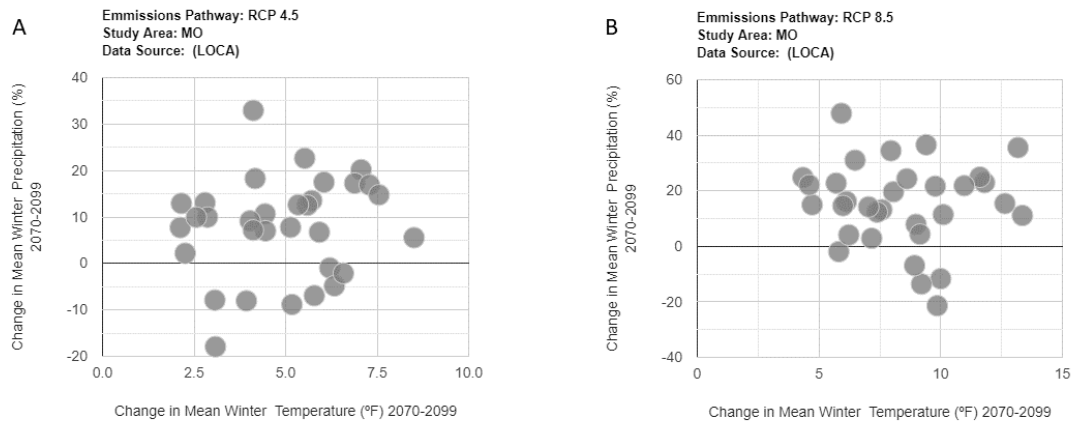


Figure 8. Same as Figure (5), but is for the Winter (DJF). Source: EPA. EPA, Environmental Protection Agency, 2021, [lasso.epa.gov/strategies](https://www.lasso.epa.gov/strategies).

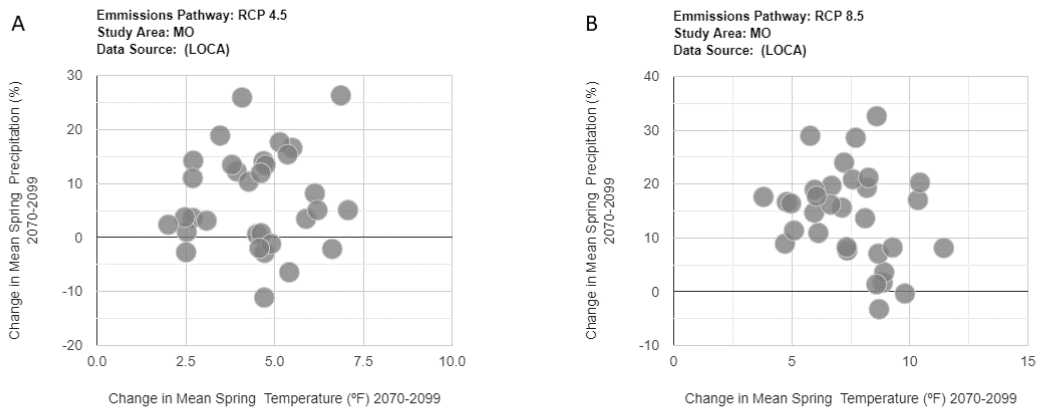


Figure 9. Same as Figure (5), but is for the Spring (MAM). Source: EPA. EPA, Environmental Protection Agency, 2021, [lasso.epa.gov/strategies](https://www.lasso.epa.gov/strategies).

## 2.2 Statistical and Dynamical Downscaling

In an attempt to look at higher resolution data for this research two separate methods can be employed, i.e., either dynamical or statistical downscaling. Using these downscaling methods involves initial data that is much coarser (100-300km) and usually data gathered from a Global Climate Model (GCM). In this study North American Regional Reanalysis (NARR) data is used as initial data that has a much higher resolution of 32km and is an extension of the National Centers for Environmental Prediction's (NCEP) Department of Energy Global Reanalysis 2 General Circulation Model Project (Mesinger et al. 2005). NARR data uses a combination of improved land surface and hydrology models and data assimilation to create a more accurate recreation of precipitation using a data set known as Parameter-elevation Regressions on Independent Slopes Model (PRISM) data (Mesinger et al. 2005). The NARR data set has forcing data available from 1979 to present and has a temporal resolution of three hours.

In order to do dynamical downscaling of this climate data, an area is selected, and physical properties such as thermodynamics and fluid mechanics, which are expected to hold under climate change, are calculated in the downscaling processes using the initial coarse dataset (GFDL, 2020; Le Roux et al., 2018). This downscaling is done using various “schemes” that tell the model what to calculate and how to use the forcing data to re-create a more detailed and higher resolution dataset. These schemes allow the downscaling process to not need observation feedback to change the model (Hou et al., 2018). This process can be very computationally expensive and is most often used in smaller areas.

Statistical downscaling is less computationally demanding compared to dynamical downscaling. When using statistical downscaling, a statistical relationship is created between

GCM coarse resolution data and local higher resolution data (Chen et al., 2010). In order to create a statistical downscaling method Van Uytven et al. (2019), talks about four general assumptions that must be made first. The assumptions are that the relationship that is being used is relevant between the predictor and predictand, the predictors are accurately simulated by the initial data, the predictand is sensitive to greenhouse gas scenarios, and the hardest to verify is that the relationship remains applicable under climate change scenarios, which is difficult because future observations aren't available. Statistical downscaling can be broken up into different categories based on how the relationships are created. The main groups are weather typing methods, stochastic methods, resampling methods, and regression methods (Chen, 2010).

### 2.3 Benefits of Regional Climate Models

With the GCMs of CMIP5 having a resolution of 70-400km it is hard to see the changes in particular precipitation events, so using RCMs are an important tool to see how particular areas may be affected by this expected change in precipitation. RCMs allow us to look at past precipitation events at higher resolutions to see how the change in urban landcover may affect the precipitation event. The state of Missouri is approximately 390km by 480km, meaning that at 400km the state of Missouri would be covered by just a little more than a single pixel at the GCM resolution. The RCM's higher resolution allows us to identify different land surfaces in the simulation that can alter precipitation amounts greatly.

When using RCMs, it becomes easier to identify finer details in the simulation such as elevation change, coast lines, smaller inland water bodies, landcover change, and temperature variation (Xu et al., 2019). Although GCMs still provide important scientific

data at a global scale, their coarse resolution makes it harder to provide meaningful data for policymakers on a regional or local scale.

In this study, the Weather Research and Forecasting (WRF) model is used to dynamically downscale lower-resolution climate data. These simulations will be used to analyze and determine if higher resolution data will follow result in similar results to GCMs. The goal is to determine if the high-resolution simulations will follow C-C equation or if it will instead follow closer to the super-C-C equation that has been proposed for lower latitude areas. Analysis will also be done to find if growing urban land cover plays a role in changes in extreme precipitation events over Kansas City.

## CHAPTER 3

### METHODOLOGY

#### 3.1 Area-of-Interest

The area of interest for this study is centered over the Kansas City metropolitan area which is separated into two separate states of Kansas and Missouri. The Kansas City metropolitan area has a population of over 2 million people and is centered in the middle of the Midwest of the United States. This area experiences atmospheric extremes during all four seasons of the year. The Kansas City area is located where the Kansas and Missouri Rivers combine and uses this river access for exporting large amounts of agricultural goods across the country. Using the Kansas City area gives us the opportunity to look at very different land cover in the same area. Over time, the Kansas City metropolitan area has continued to stretch farther out from its core creating large areas of impervious surfaces.

#### 3.2 WRF and Parameters

For this study on extreme precipitation events, the WRF model was utilized. WRF is a mesoscale numerical model developed by the National Center for Atmospheric Research (Skamarock et al. 2008). WRF is comprised of two dynamical solvers known as Advanced Research WRF (ARW) core and Nonhydrostatic Mesoscale Model (NMM) core. The WRF model has various parameters that can be changed for different atmospheric processes. These parameters have been created to help simulate different atmospheric conditions and allows users to tailor the model to their needs. The physics schemes that were used in the simulations are shown in Table 1. These physics schemes were chosen after a suite of sensitivity experiments were ran on precipitation events in the area for a separate study. These schemes provided the best results for recreating precipitation events within the area of

interest. The Kain-Fritsch cumulus scheme was used in the outer most domains only since convection can be resolved at resolution higher than 3km.

Table 1. Shows the parameters used for all simulations in this study. All parameters were used across all domains of the simulation except for Cumulus which was used in the outer 2 domains only.

Parameter Option	Parameter Name	References
MP_physics	Thompson	Thompson et al. 2008
RA_LW_physics	RRTMG	Lacono et al. 2008
RA_SW_physics	RRTMG	Lacono et al. 2008
Surface layer	Eta	Monin and Obukhov 1954, Janji 1994, 1996, 2002
Land surface model	Noah	Tewari et al. 2004
PBL physics	MYNN3	Nakanishi and Niino 2006, 2009 Olson et al. 2019
Cumulus physics	Kain-Fritsch	Kain 2004

### 3.3 Model Setup

#### 3.3.1 Initial Data

The initial conditions data set used for this study was the North American Regional Reanalysis (NARR). NARR was created by NOAA's National Center for Environmental Prediction (NCEP) as an extension to their Global Reanalysis project. NARR data uses the high resolution NCEP of 32km paired with the Regional Data Assimilation System to increase accuracy of variables such as temperature and precipitation.

#### 3.3.2 Domains

In order to obtain the resolution required for analysis of precipitation, three nested domains were created. Within the WRF model, the domains' resolutions bring the 32km resolution NARR data to 9, 3, and 1 km resolutions with the inner most domain at 1km centered over the Kansas City Metropolitan Area. Figure 10 shows an elevation map with the domains drawn. The simulation is set up to have the atmospheric data split into 44 separate layers to better handle the atmospheric changes that occur during extreme precipitation events. The simulation also splits the ground into 4 separate layers to better reproduce ground water levels during the precipitation event. The inner-most domain shown in Figure 12 is the area of focus in this study, however, data from domain 2, shown in Figure 11, will be analyzed to obtain larger area of precipitation to compare. Using the second domain will not show as much land cover change between the separate time periods due to the lower resolution and the area being dominated by largely undeveloped farm and grasslands.

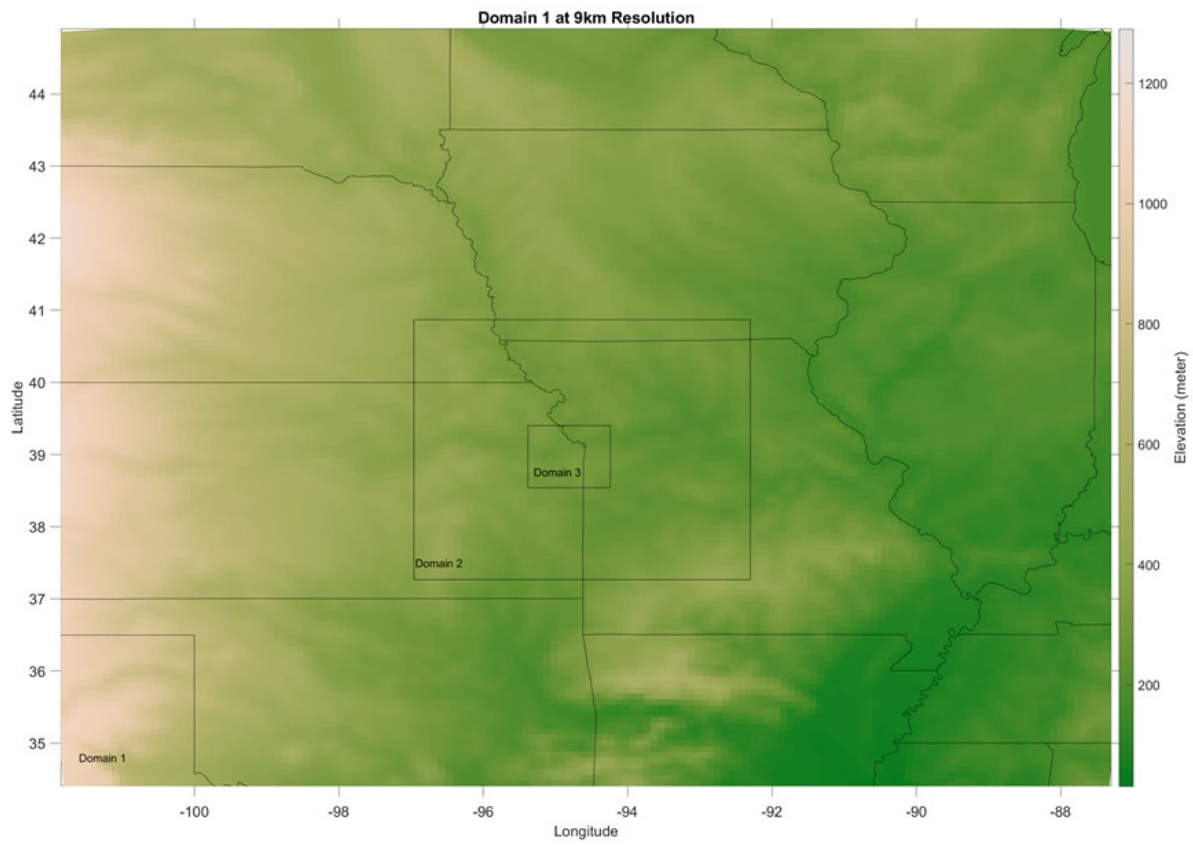


Figure 10. Shows the topography of domain 1 used for both historic and present-day simulations. Domains 2 and 3 are also drawn and labeled. This domain is at a 9km resolution.

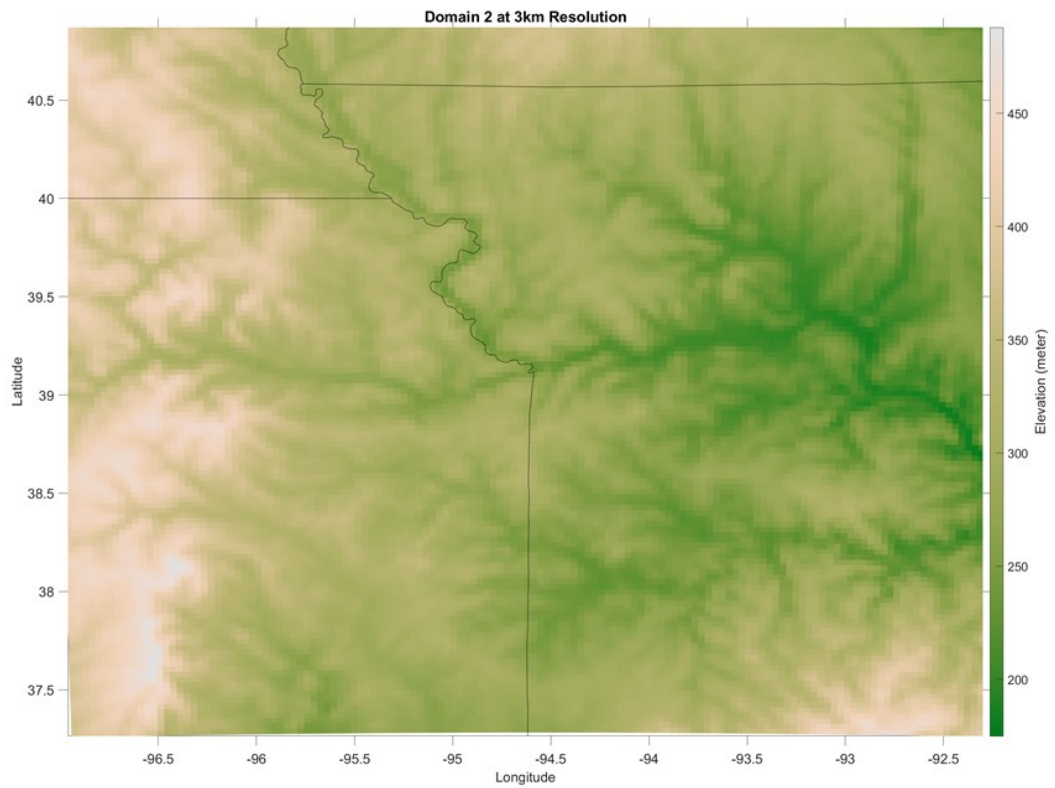


Figure 11. Shows domain 2 topography at 3 km resolution after being interpolated from domain 1. This is the coarsest resolution that will be analyzed for this study.

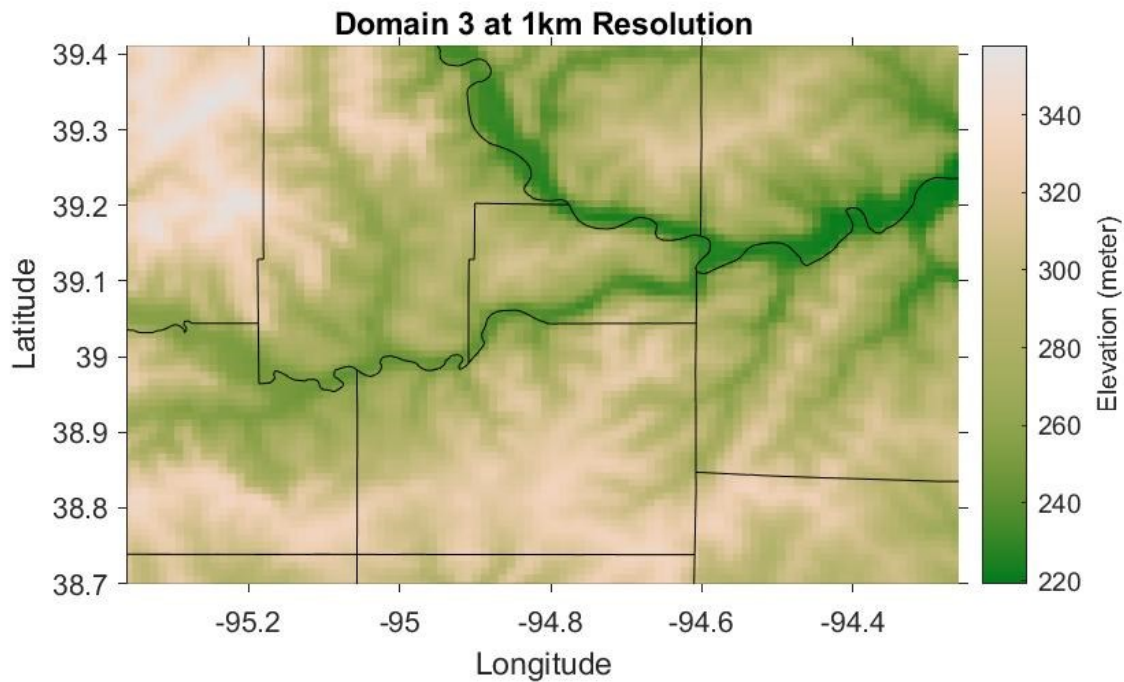


Figure 12. Shows the inner most domain (domain 3) for this study that has a 1km resolution. This is the primary domain that will be analyzed and is centered over the greater Kansas City area.

### 3.3.3 Land Cover for 2016 Simulation

This study looks at the extreme event of Winter Storm Ulmer that happened in March 2019. The land cover that was used for this simulation was from 2016, which provided accurate landcover for the present-day simulation for the event. Having accurate landcover was important to see so that a comparison in precipitation could be made between the present-day and historic landcover. The 2016 land cover was readily available and would make a fair representation of present-day land cover. The land cover for 2016 can be seen in

Figure 13 and shows the urban land cover for 2016. The large area of low intensity residential area represents the surrounding suburban areas that have taken the place of what used to be grass and wetlands.

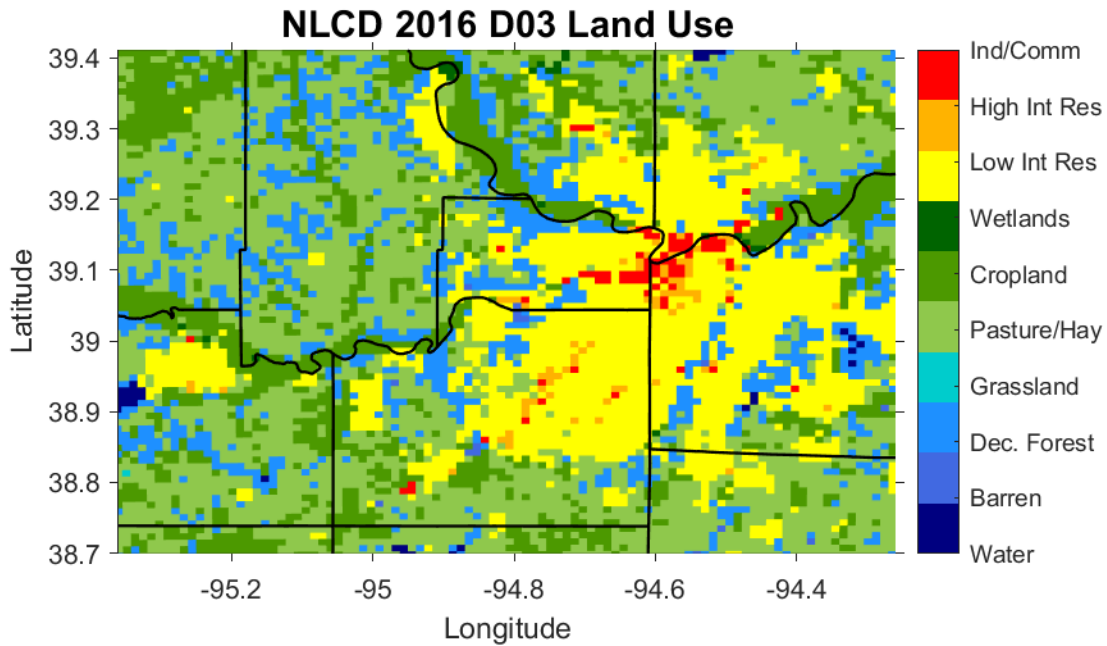


Figure 13. Shows the land cover map for the Kansas City region at a 1km resolution in 2016.

### 3.3.4 Land Cover for 1938 Simulation

In this study, two different land covers are used to compare the effects of urban land cover on extreme precipitation events. The second data set used was determined by the earliest data available, which was from the year 1938. This data was created by the United States Geological Survey using the Forecasting Scenarios of Land use Change (FORE-SCE) model. The initial conditions for this model were created using the land use and land cover (LULC) and started in 1992 and created a backcast simulation to get historical land cover

(Sohl et al., 2016). The land cover data was 250m resolution from 1938 to 1992 (Sohl et al., 2016). This land cover shown in Figure 14 shows the greater Kansas City area before massive development occurred. The 1938 land cover shows the lack of industrial development or high intensity residential areas. In 1938, a majority of the domain was either pasture or cropland. In the southern portion of the domain the area was once largely covered in grass and wetland areas.

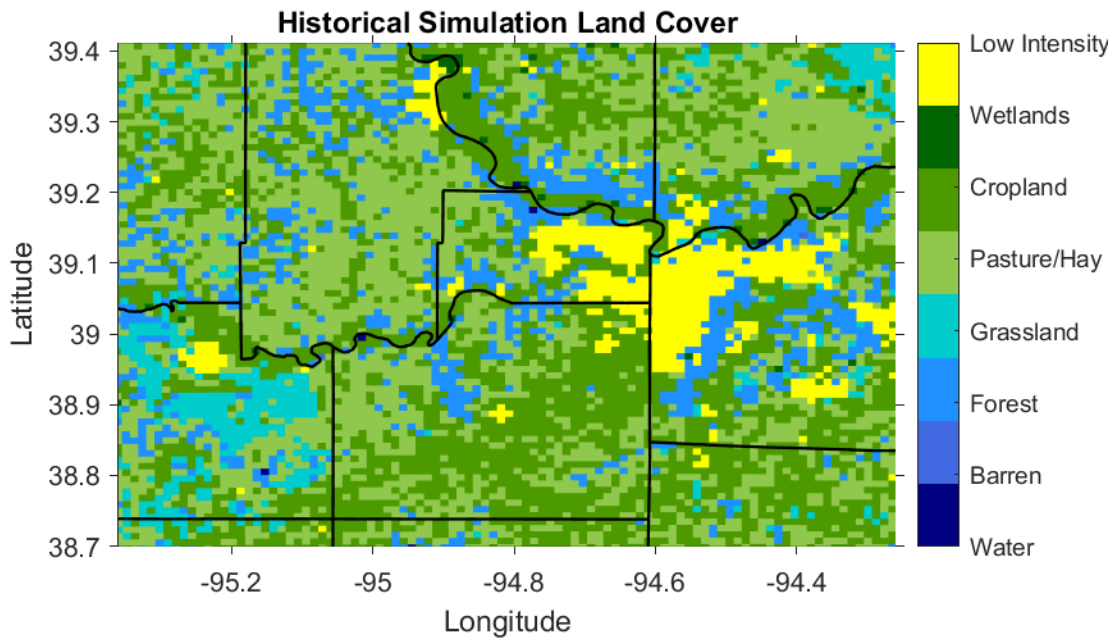


Figure 14. Land cover map 1938 over Kansas City at a 1km resolution. This map shows the predicted land cover for Kansas City in 1938 based off the FORE-SCE model. The key

differences from the 2016 land cover are the lack of high intensity land cover, lack of urban sprawl, and greater areas of grassland.

### 3.3.5 Observational Analysis

The first step after the initial control simulations were ran for both the present-day and historic landcovers was to compare the simulations to observational data acquired from the Midwest Regional Climate Center (MRCC). The MRCC data was taken from five separate weather stations around the Kansas City area on both the Missouri and Kansas side. The stations chosen shown in Figure 15 are the Kansas City International Airport (MCI) at  $39.2972^{\circ}$  N and  $-94.7306^{\circ}$  W, Downtown Kansas City Airport at  $39.1208^{\circ}$  and  $-94.5969^{\circ}$ , Lee's Summit Airport at  $38.9597^{\circ}$  and  $-94.3714^{\circ}$ , New Century Air Center at  $38.8317^{\circ}$  and  $-94.8897^{\circ}$ , and Johnson County Executive Airport  $38.85^{\circ}$  and  $-94.7392^{\circ}$ . These weather stations were chosen to look at the observational data to compare with the daily outputs and total precipitation values of the control simulations. This analysis will be to understand how the recreated precipitation differed from observed data.

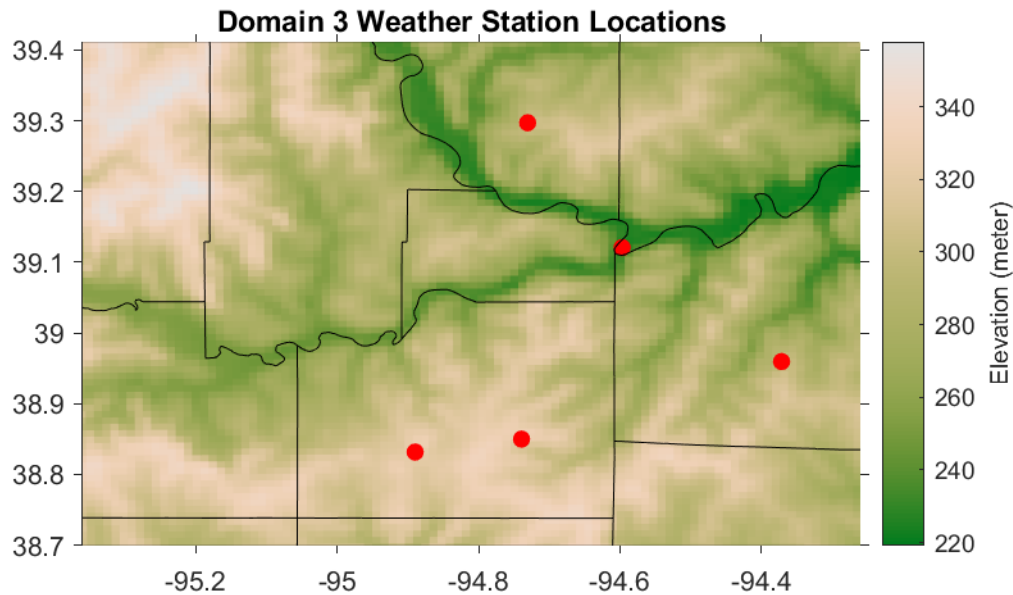


Figure 15. Domain 3 at a 1km resolution with the locations of the weather stations used for the observational analysis. The Kansas City International Airport (MCI) at 39.2972°, -94.7306°, Charles B Wheeler Downtown Airport at 39.1208° and -94.5969°, Lee’s Summit Airport at 38.9597° and -94.3714°, New Century Air Center at 38.8317° and -94.8897°, and Johnson County Executive Airport 38.85° and -94.7392°.

### 3.3.6 Sensitivity Experiments

The sensitivity experiments for this study were done by changing the temperature values for the simulation to show the difference in precipitation from a past event with an increase and decrease in temperature values. After the initial simulation were ran using both the 2016 and 1938 land cover, the intermediate files were created for both land cover simulations. These intermediate files are files created by WRF combining the NARR forcing

data and land cover to create a series of files for use in the downscaling process. The next step was done by creating separate intermediate files and to alter all temperature values across every atmospheric level either +1°, +2°, -1°, or -2°C. These files were then reinserted into the WRF model to be ran using the new temperature values for the same time period using the same settings as the control simulations.

### 3.3.7 Experimental Design

Once initial conditions are set for the simulation, the control simulation was ran to establish a base line for the precipitation event of winter storm Ulmer between March 3 – 17, 2019. The first four days of the simulation were used as a spin up period to establish a more stable simulation during the event. This spin up period had very little precipitation and was removed from the data analysis. The baseline simulations were ran for the 2016 land cover as well as the unaltered temperature 1938 land cover before starting the suite of sensitivity experiments.

The next step was to run the four sensitivity experiments for the present day and historical land covers. This gave four sensitivity experiments for each land cover (-2°, -1°, +1, +2°C) to compare both precipitation values and temperature change. The historic land cover sensitivity simulations temperature changes are compared to the present-day sensitivity simulations temperature values. These temperatures were not scaled off preindustrial levels that have been used in some IPCC studies. This was done so that the initial control simulation from 2019 was not altered in any way to get the best present-day re-creation of precipitation possible. Analysis will be done in both the 2<sup>nd</sup> and 3<sup>rd</sup> domains at 3 and 1km resolution. The values were taken from domain 2 to look at a wider area to get a larger area

of precipitation to analyze; however within the 2<sup>nd</sup> domain there was much less change in the land cover between urban and non-urban areas.

## CHAPTER 4

### RESULTS

#### 4.1 Observational Analysis of 2016 Control

To look at the control simulation accuracy, the coordinates are taken for five different airports inside the inner most domain. These airports are the Kansas City International Airport (MCI), Charles B. Wheeler Downtown Airport (MKC), Lee's Summit Municipal Airport (LXT), Johnson County Executive Airport (OJC), and New Century Air Center (IXD). All the airports that will be used in this analysis have weather stations on site and the data was collected from the Midwestern Regional Climate Center (MRCC) database that consists of around 850 weather stations across the United States. Daily precipitation data was downloaded from the MRCC and then compared to daily output of the control simulations.

Looking at Figures 16-20, it shows that while the precipitation is falling on the correct days, the totals are different. Further investigation was done into the point analysis shown on Table 2 where the totals over the simulated time were compared, which shows the simulation has more rain at each weather station. This total comparison shows that precipitation values are hard to re-create at such a high resolution. Having slight changes in the precipitation pattern can drastically change the precipitation totals given the 1km resolution compared to the size of the weather stations.

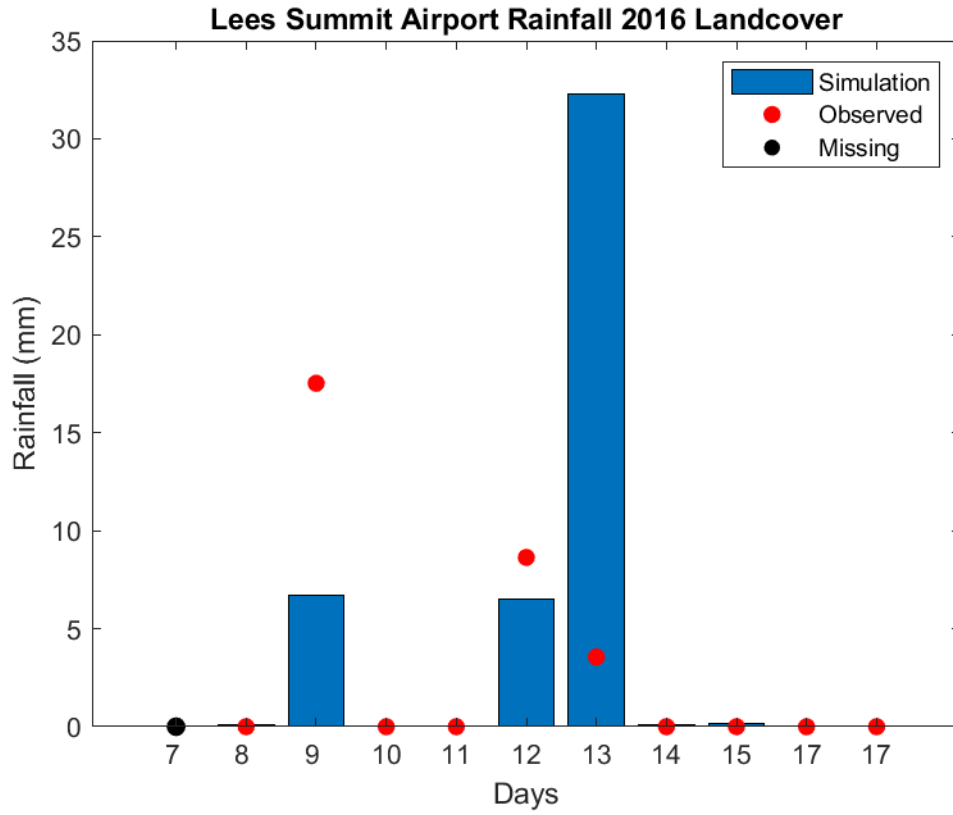


Figure 16. Daily precipitation values for the simulation and observed data at the Lee's Summit airport with the present-day landcover.

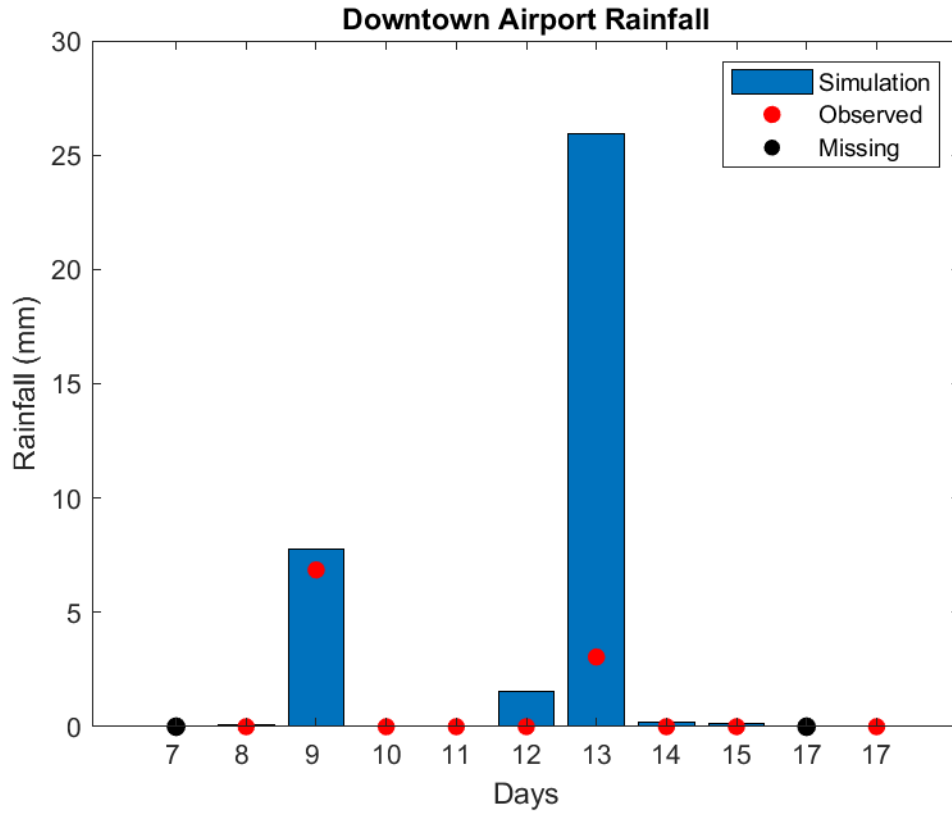


Figure 17. Daily precipitation values for the simulation and observed data at the Downtown Kansas City airport with the present-day landcover.

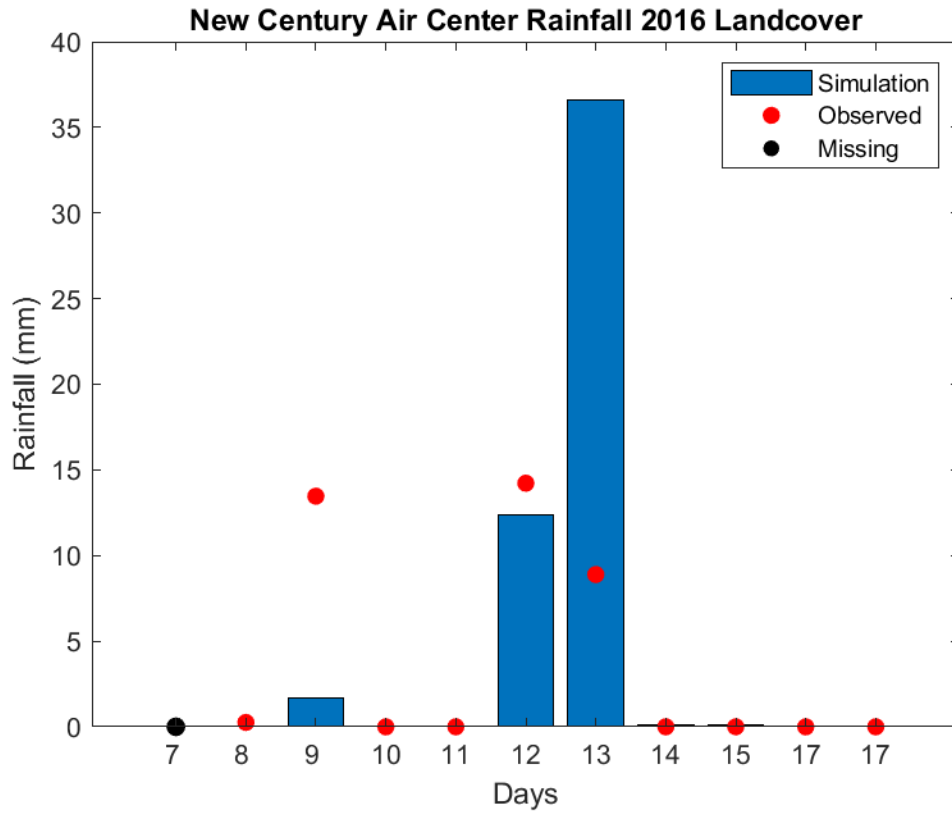


Figure 18. Daily precipitation values for the simulation and observed data at the New Century Air Center airport with the present-day landcover.

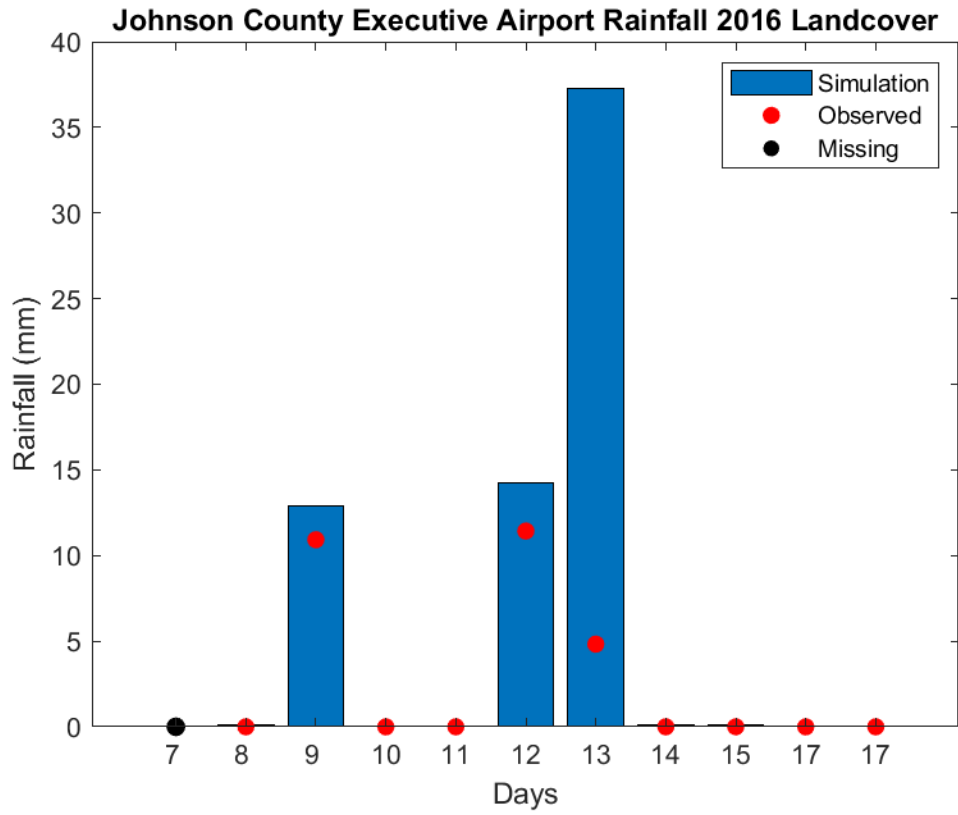


Figure 19. Daily precipitation values for the simulation and observed data at the Olathe airport with the present-day landcover.

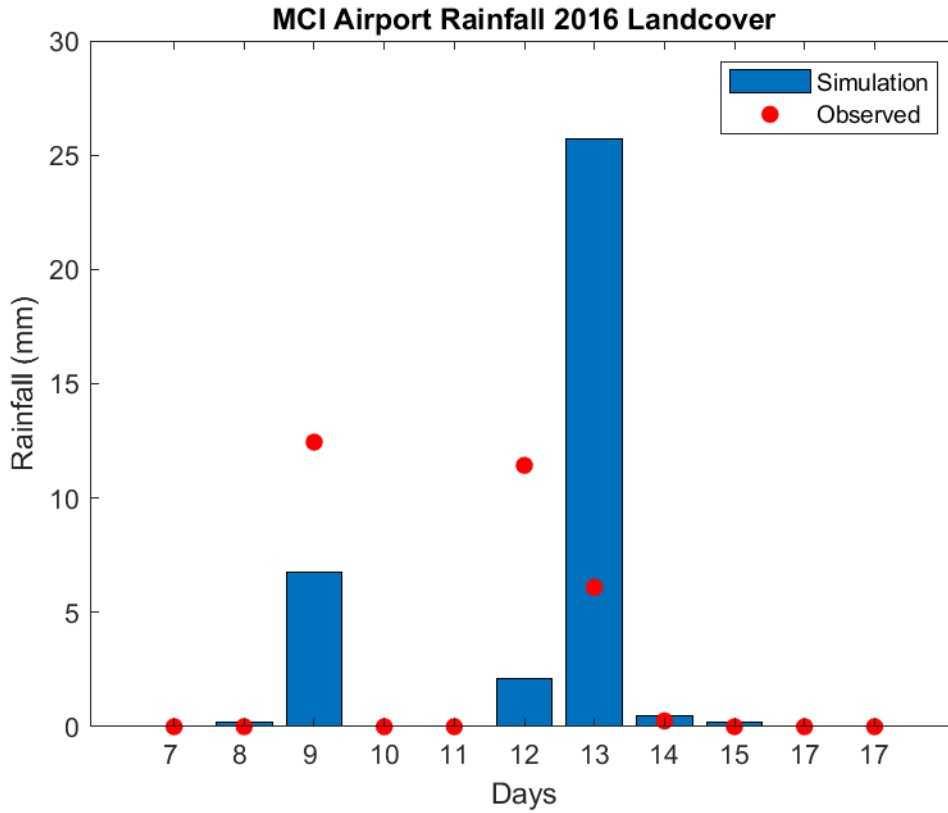


Figure 20. Daily precipitation values for the simulation and observed data at the Kansas City International airport with the present-day landcover.

Table 2. Precipitation totals for each weather station site for both the observed data and the present-day simulation.

Observed vs Present-day Simulation Weather Station Comparison					
Johnson County					
	Downtown	Lee's Summit	Executive Airport	New Century Air Center	MCI
Observed	9.91mm	29.72mm	27.18mm	36.83mm	30.23mm
Present-day	35.68mm	45.83mm	64.81mm	50.93mm	35.47mm

#### 4.1.2 Analysis of the Initial Simulations

Control simulations were ran from March 3-17, 2019 using the parameters mentioned in Table 1. The first four days of the simulation were used as spin up time and were not used for analysis of any data. For this study, two separate simulations were created using identical initial conditions except for the landcover. The landcover for the 2016 simulation is shown in Figure 13 and the land cover for the 1938 simulation is shown in Figure 14. The initial analysis of these control simulations was to see if change occurred within the precipitation totals based solely on the landcover change. Results for both the 2<sup>nd</sup> and 3<sup>rd</sup> domain are shown in Figure 21. These domains do not give one definitive number to determine if one of the controls had more precipitation than the other, so an average of all pixels was taken to see the average percent change and what that percent change translates into for mm of precipitation shown in Table 3. The averaged precipitation change between the different controls shows a very similar amount of precipitation overall.

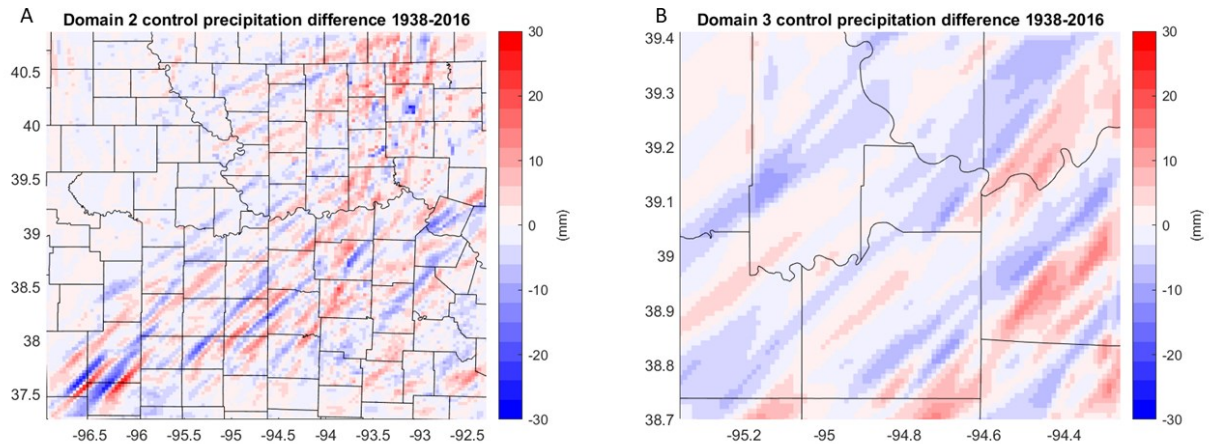


Figure 21. Pixel-to-pixel comparison taking the 2016 precipitation values from the 1938 control simulation for the 2<sup>nd</sup> domain (A) and 3<sup>rd</sup> domain (B).

Table 3. Shows the percent change and average change found over the entirety of domains 2 and 3 between the initial simulations of 1938 and 2016.

Precipitation Change between Control Models		
	Domain 2	Domain 3
Percent Change	0.0036%	-0.0085%
Average Change	0.17mm	-0.37mm

The comparison of domain 3 at 1km resolution for both control simulations is presented in Figure 22. The temperature data is an averaged value for each pixel from March 7-17. The control comparison shows a clear increase in temperature for the present-day simulation even showing a distinct outline of Leavenworth, KS and Lawrence, KS outside of the Kansas City area. The 2<sup>nd</sup> domain was not used for temperature analysis because the

larger domain is made of primarily undeveloped farmlands. The average change in temperature over the Kansas City area shown in Table 4 is not very large, however a much more significant temperature change in the Kansas City core lines up closely with the historic landcover extent shown in Figure 14.

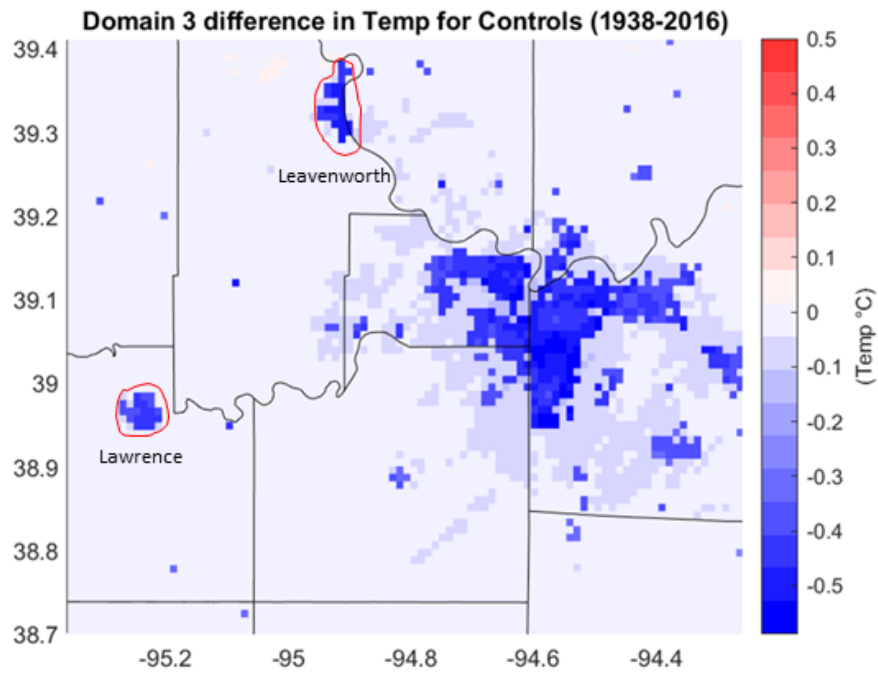


Figure 22. Shows the difference between the 1938 and 2016 initial simulations' averaged temperatures over the entire simulation. Leavenworth is shown northwest of the Kansas City area and Lawrence is shown to the west.

Table 4. Percent change and mean difference between both control simulations.

Temperature Change for Control Models	
Domain 3	
Percent Change	Mean Change
-0.016%	-0.043°C

## 4.2 Sensitivity Simulation Results

### 4.2.1 Precipitation Results for 2016

The goal of the initial simulation with 2016 the landcover was to re-create the most accurate simulation possible for the time of the event in 2019. This 2016 landcover has much more urban sprawl than the 1938 landcover and has developed commercial and industrial areas near the Missouri River. For this portion of the study, sensitivity experiments were set up where the temperature over all domains was either increased or decreased by one or two degrees Celsius. Once the sensitivity models were ran, the precipitation data was compared to the respective initial simulation. Figures 23 and 24 show the precipitation differences from the control for both domain 2 and 3. When the sensitivity experiments were compared, all domain 3 sensitivities exceeded the expected C-C equation's 7% increase except for the increase of one degree shown in Table 5. The second domain was analyzed to give a larger sample size and to account for the change in precipitation patterns. These results exceeded the same expectations as domain 3 in every sensitivity simulation. All the exceeded simulation results are closer to 12-14% per degree increase which is much closer to the super-CC scaling discussed earlier (Shown in table 5).

Table 5. Percent change and average precipitation difference for each sensitivity simulation for 2016 compared to the control.

2016 percent change from control					
Temperature	-2	-1	Control	1	2
Domain 2	-20.54%	-11.51%	45.54mm	13.75%	28.99%
Domain 2	-9.35mm	-5.24mm		6.26mm	13.20mm
Domain 3	-21.13%	-12.73%	43.36mm	7.32%	12.86%
Domain 3	-9.16mm	-5.52mm		3.18mm	5.58mm

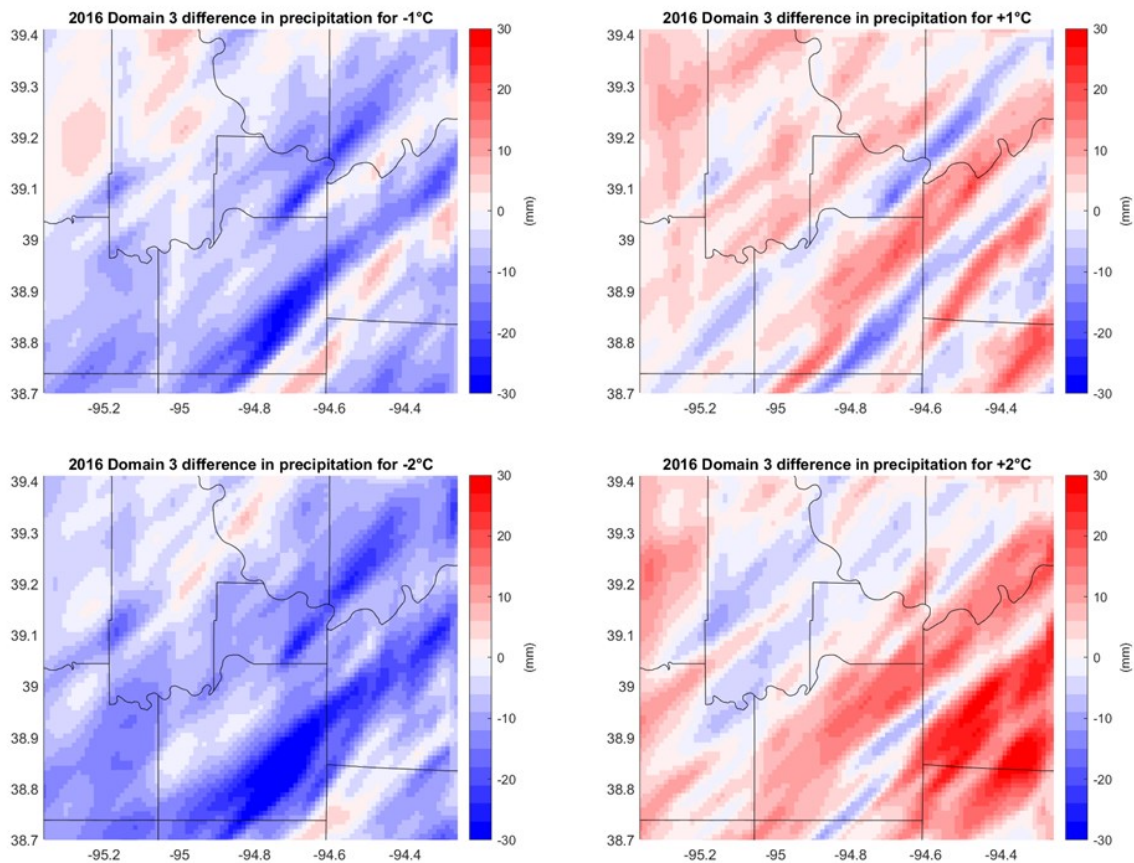


Figure 23. Difference in precipitation for each sensitivity experiment compared to its 2016 landcover control simulation in Domain 3.

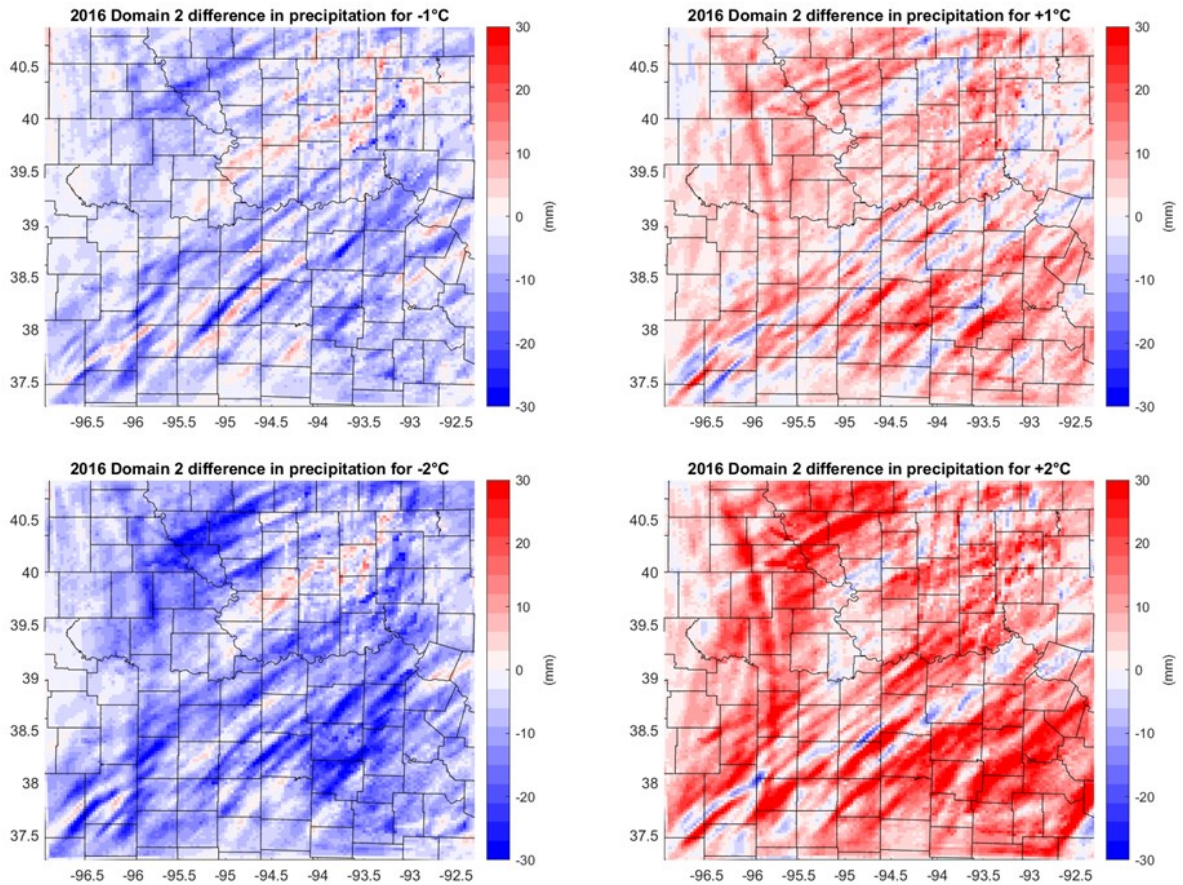


Figure 24. Precipitation difference between the 2016 control and the sensitivity simulations in Domain 2.

#### 4.2.2 Precipitation Results for 1938

The second set of sensitivity simulations ran were made using the same atmospheric forcing data as the 2016 landcover but instead had the estimated 1938 landcover Figure 14. In this simulation, there is no high intensity or industrial/commercial land cover as was found in the 2016 simulation. This landcover has significantly less low intensity land use and urban sprawl compared to the previous simulations as well, and grasslands are more prevalent in surrounding areas (Figure 13). Figure 25 shows the difference in precipitation for each

sensitivity experiment compared to the control simulation, while Table 6 shows the average precipitation difference and the percent change from the control domain. The 1938 landcover average percent change shown in Table 6 shows all sensitivity simulations have less of a difference from the control when compared to the 2016 simulations except for the +1°C and the 2<sup>nd</sup> domain for +2°C simulations.

Table 6. Percent change and average precipitation difference for each 1938 sensitivity simulation from the control.

Temperature	1938 percent change from control				
	-2	-1	Control	1	2
Domain 2	-19.69%	-10.56%	45.64mm	14.28%	30.30%
Domain 2	-8.99mm	-4.82mm		6.52mm	13.83mm
Domain 3	-20.62%	-10.09%	42.95mm	10.03%	12.31%
Domain 3	-8.86mm	-4.33mm		4.31mm	5.29mm

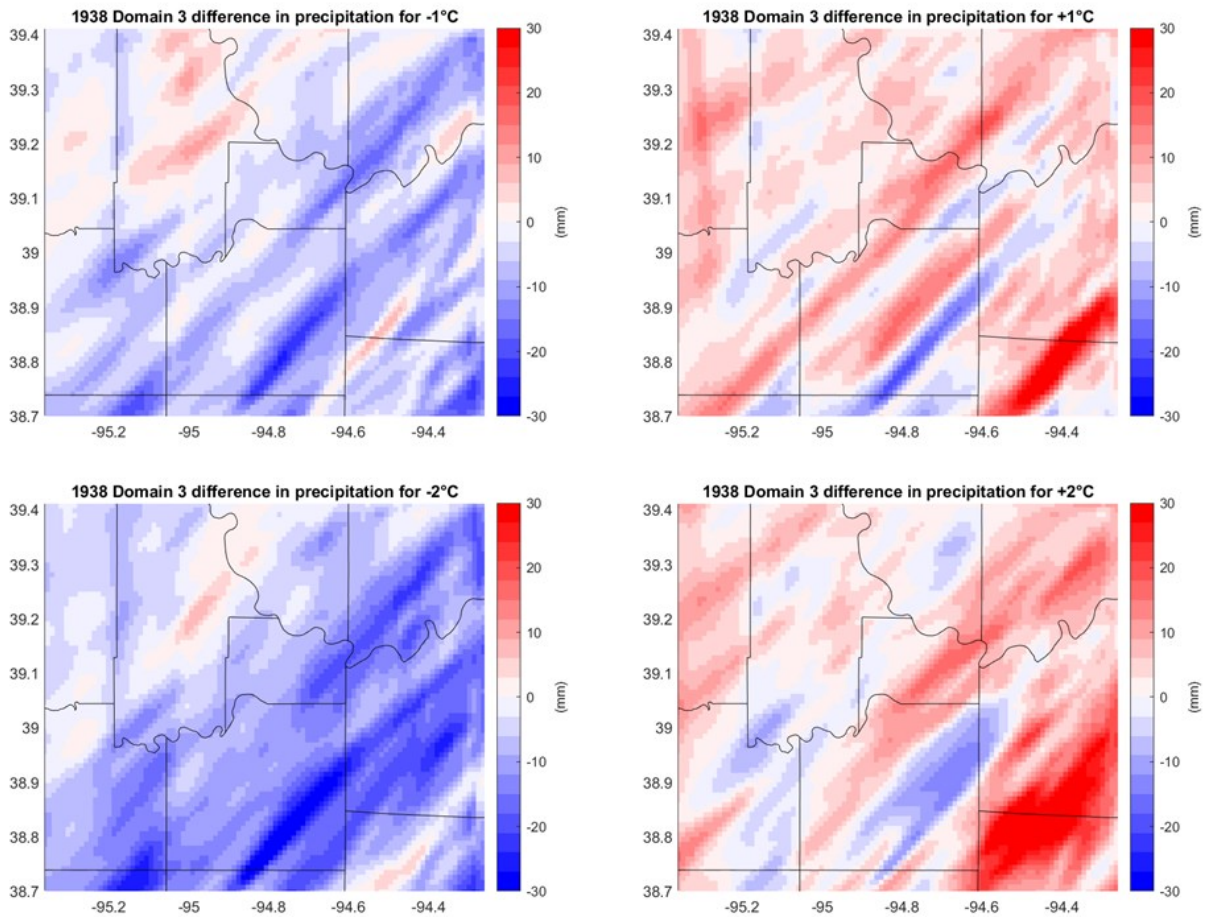


Figure 25. Difference in precipitation for each sensitivity experiment compared to its 1938 landcover control simulation in Domain 3.

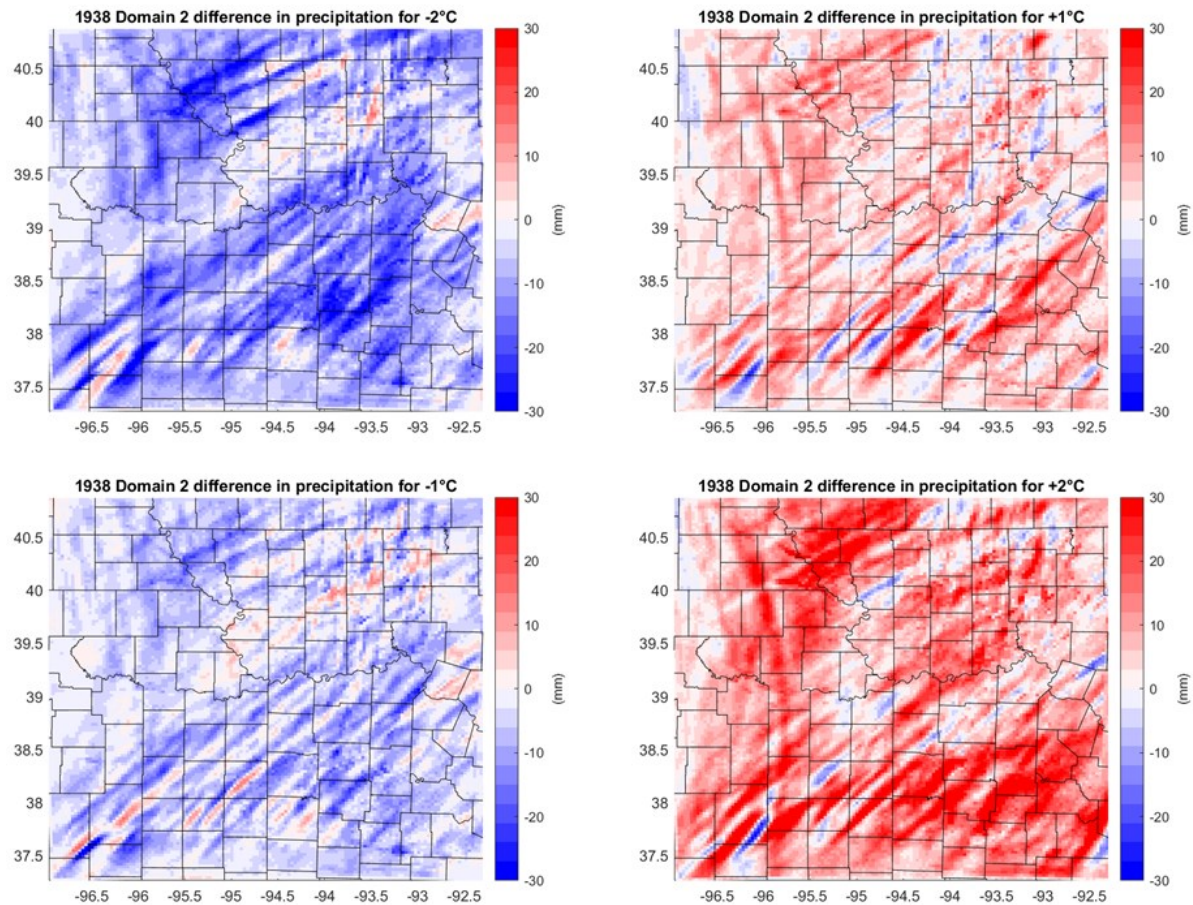


Figure 26. Precipitation difference between the 1938 control and the sensitivity simulations in Domain 2.

#### 4.2.3 Temperature Analysis for 2016

After all sensitivity simulations were complete for 2016, the spin up days were removed from the data and the T2 values were averaged for each pixel for the entire simulation. These averaged T2 values were subtracted from the original simulation's averaged T2 values to evaluate the effect of the changed landcover and temperature values. In Figure 27, these difference values have been plotted for domain 3 where the clear outline of the urban landcover can be observed. Results from domain 2 were not analyzed because

the area surrounding the Kansas City area is largely farm and grasslands with relatively low urban development.

With the forcing data manipulated to increase and decrease the temperature across the domains by 1 and 2°C the averaged temperature change was examined to see how this would be affected over the entire simulation during a large precipitation event. In Table 7, the average temperature change over domain 3 increased by roughly 0.60°C for each incremental increase for the sensitivity simulations. The absolute maximum value was taken from within domain 3 and is shown within Table 7. These maximum values more closely follow the degree increase for each simulation.

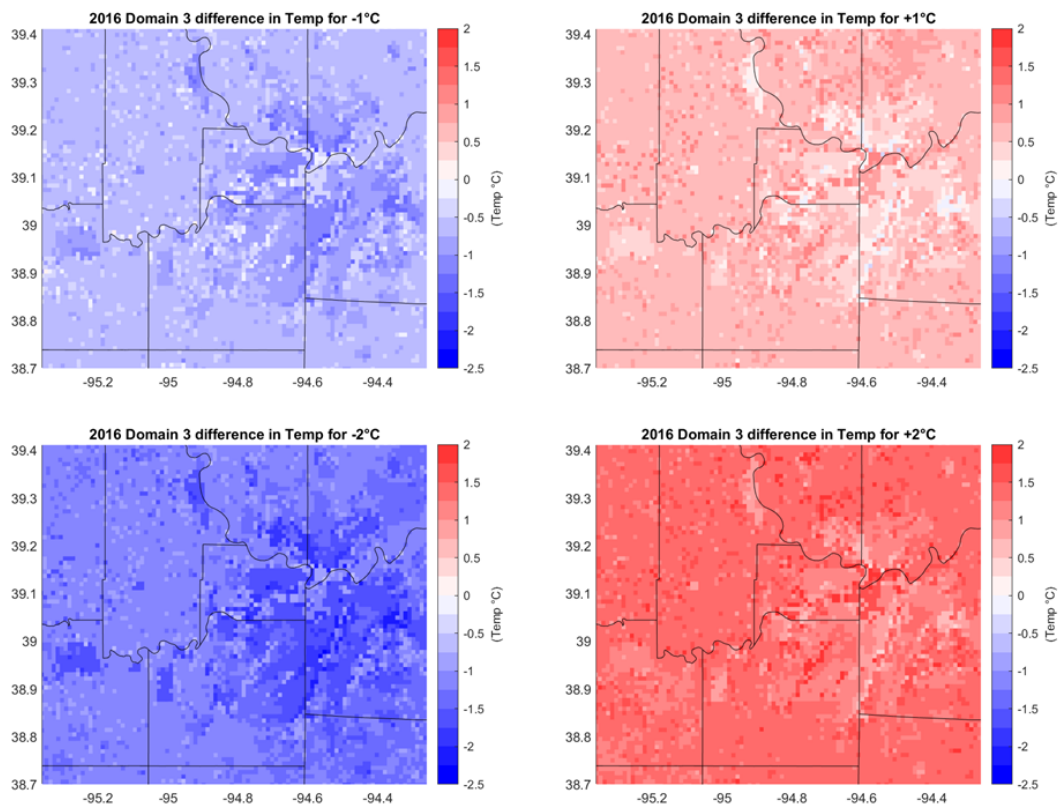


Figure 27. Difference in averaged T2 values for each point in the 2016 sensitivity simulations in domain 3 compared to the control simulation.

Table 7. The first row shows the average temperature difference from the control simulation for each 2016 sensitivity simulation. The second row shows the largest absolute average temperature difference found for each sensitivity simulation.

Temperature	2016 T2 difference from control			
	-2	-1	+1	+2
Tavg	-1.27°C	-0.64°C	+0.64°C	+1.32°C
Tmax	1.35°C	0.77°C	1.34°C	2.04°C

#### 4.2.4 Temperature Analysis for 1938

The analysis of T2 from the 1938 sensitivity simulations show similar results to the 2016 simulations when averaged over the entire domain (Table 8). The urban areas are clearly identifiable in all sensitivity difference analyses except for the -1°C simulation. The -1°C simulation has a blanket cooling effect over the entire area instead of showing the urban heat island effect shown in Figure 28. The averaged temperature change over all sensitivities were about 0.6°C per 1°C changed on the initializing data.

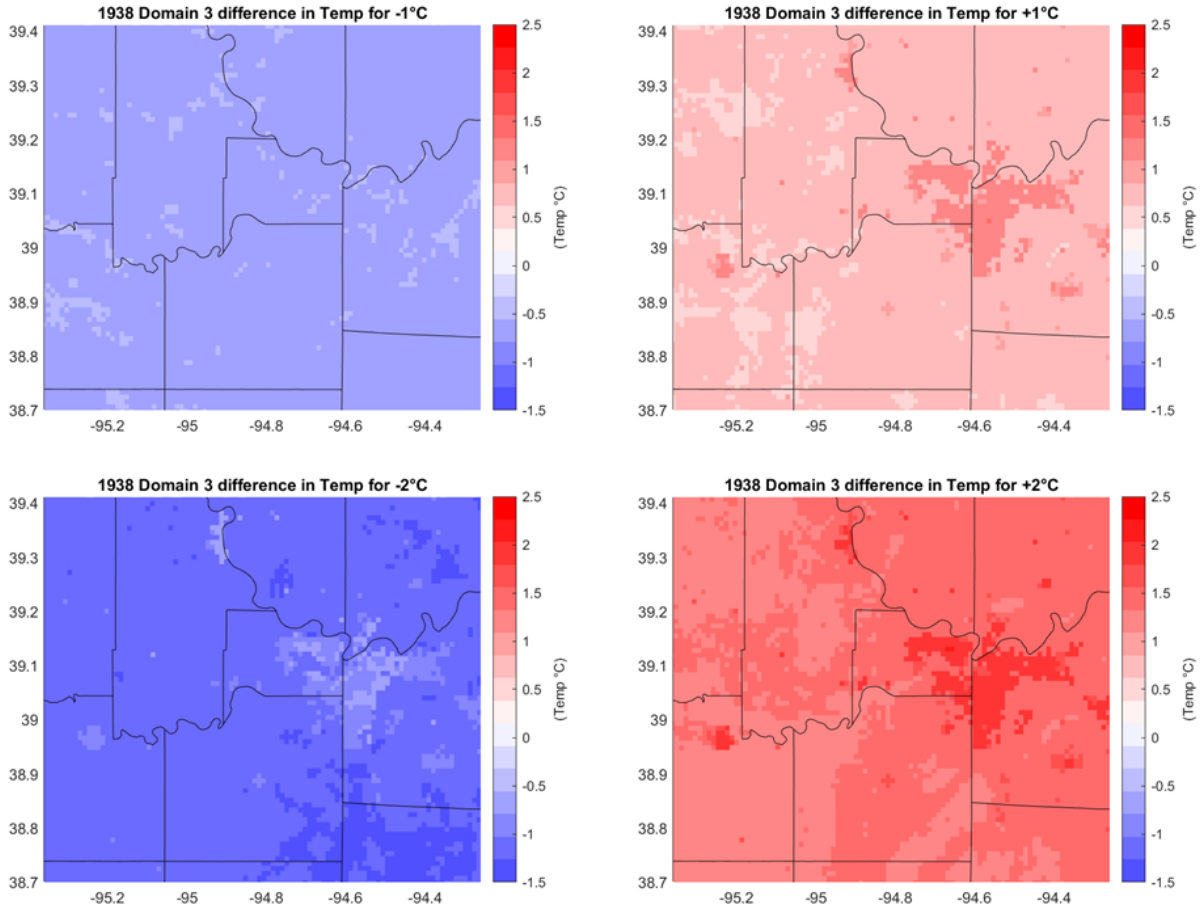


Figure 28. Difference in averaged T2 values for each point in the 1938 sensitivity simulations in domain 3 compared to the control simulation.

Table 8. The first row shows the average temperature difference from the control simulation for each 1938 sensitivity simulation. The second row shows the largest absolute average temperature difference for each sensitivity simulation.

1938 T2 change from control				
Temperature	-2	-1	1	2
Tavg	-1.19°C	-0.60°C	+0.69°C	+1.36°C
Tmax	2.31°C	1.57°C	1.30°C	1.96°C

### 4.3 Joint Analysis

The next step for analysis was to get a comparison between the historic and present day landcover simulations. The 2016 landcover has a much larger urban footprint compared to the 1938 landcover. These simulations had the same model parameters except for landcover. The goal of this analysis was to look at how the landcover would affect not only the precipitation of this event, but also how the average temperature would change.

#### 4.3.1 Precipitation Analysis Between 1938 and 2016 Simulations

In this analysis each sensitivity experiment for the present-day simulation was subtracted from the respective historic sensitivity simulation. This allowed calculations of how much of a difference there was based solely off the change in landcover for each degree increase/decrease from baseline. When analyzing the plotted data in Figures 29 and 30, it is difficult to tell which simulation set had a larger amount of precipitation. To get a better understanding of the difference in precipitation, an average was taken over the difference of each difference data set, which is shown in Table 9. In domain 2, the 1938 simulation shows a greater percent change in precipitation across all sensitivity simulations. In domain 3, the extreme sensitivity simulations of -2 and +2 show a greater percent change in precipitation for the 2016 simulation.

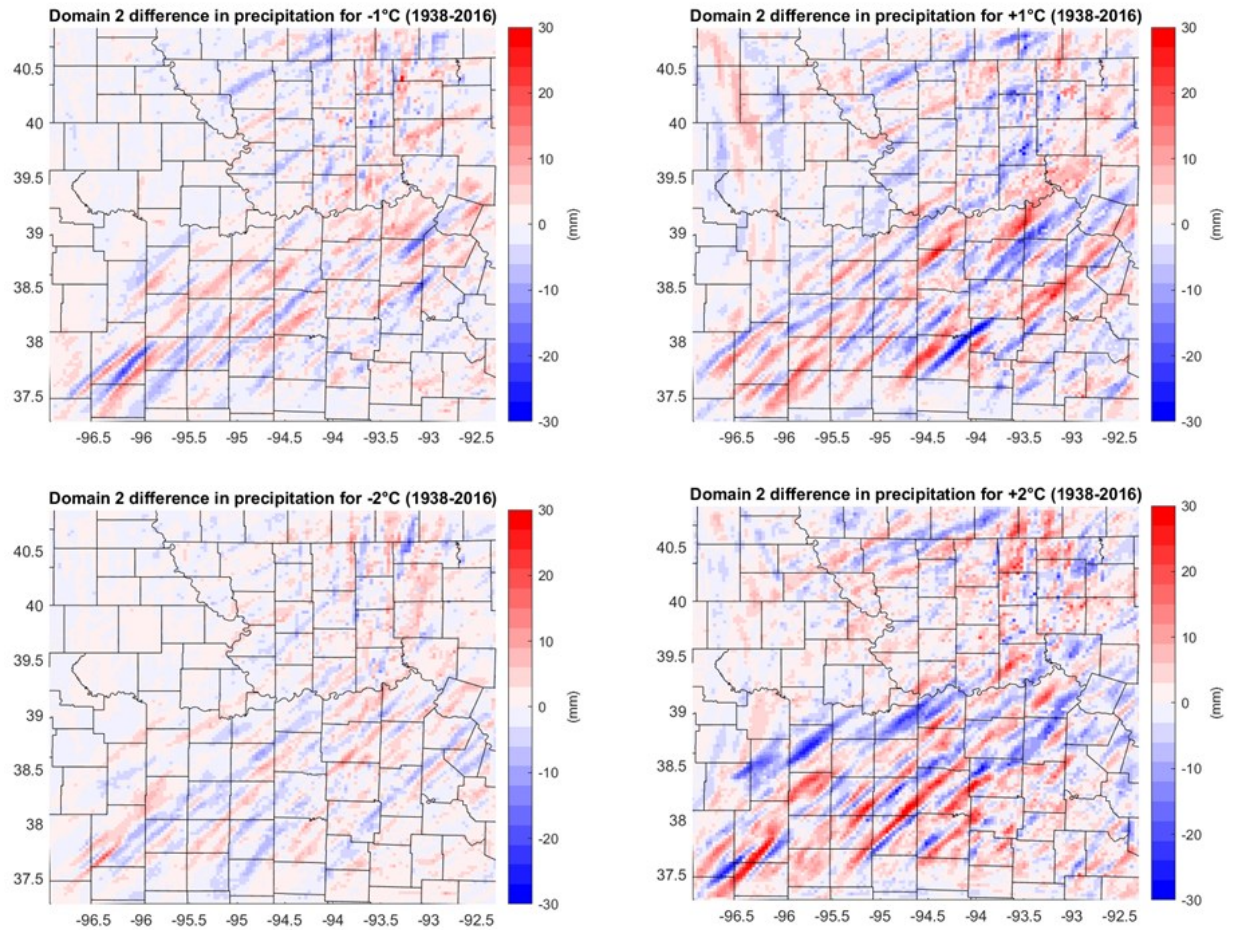


Figure 29. Precipitation difference for each sensitivity simulation in domain 2 between 1938 and 2016.

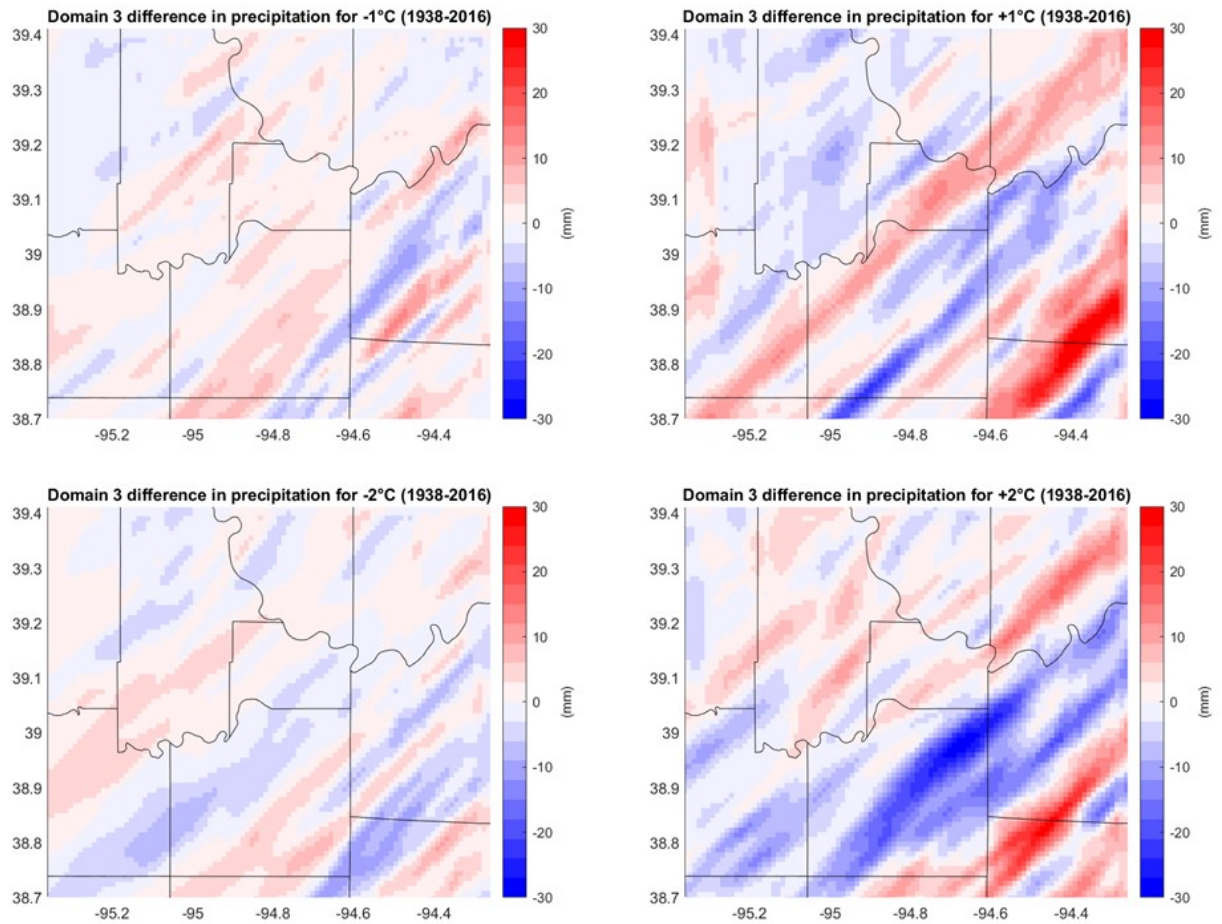


Figure 30. Precipitation difference for each sensitivity simulation in domain 3 between 1938 and 2016.

Table 9. The average percent change between historic and present-day sensitivity simulations. Negative values show a greater precipitation value in the 2016 sensitivity simulations.

	Joint Analysis Difference (1938-2016)			
	-2	-1	1	2
Domain 2	2.06%	0.94%	0.70%	1.18%
Domain 3	-0.30%	2.27%	2.06%	-0.75%

#### 4.3.2 Temperature Analysis

When comparing the historic to present-day sensitivity simulations the T2 values were evaluated and are shown in Figure 31. When analyzing the sensitivity simulation comparisons, you can see an increase across all sensitivities in the Kansas City core where the high intensity and industrial landcover is found in the 2016 simulations. In the surrounding areas where the 2016 landcover has suburban development, the historic simulations show higher T2 values. In Table 10, results are shown for the average change for the 1938 simulation compared to their respective 2016 sensitivity simulations. These results show that while the heat distribution has been changed by urban landcover change, the change has remained constant. In the -1°C sensitivity simulation you can see a clear outline of where the high-intensity residential and industrial landcover are located in the 2016 simulations. The absolute difference shown in Table 10 shows the largest value change in overall sensitivity simulations.

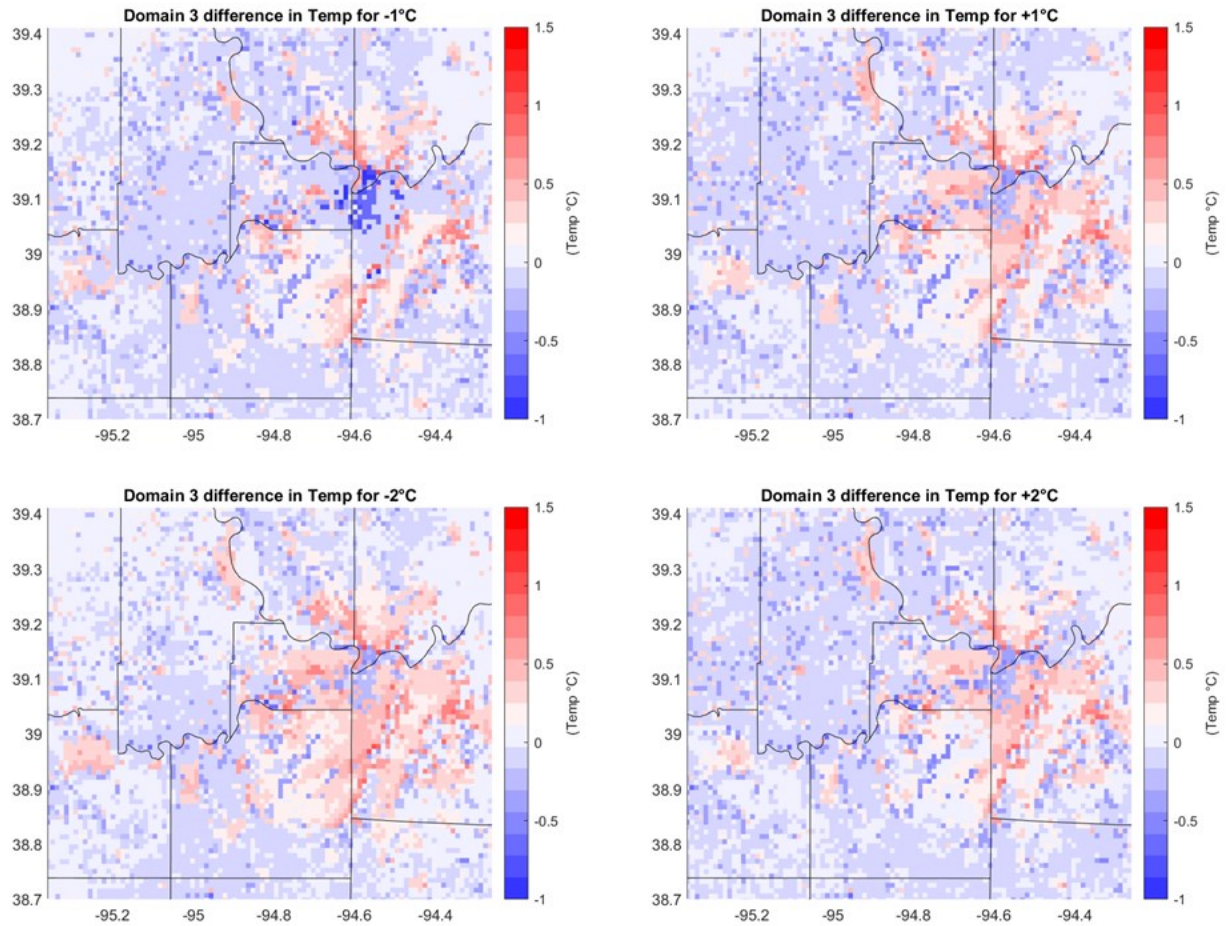


Figure 31. Shows the difference between the mean temperature difference of each sensitivity simulation for 1938 and 2016 landcovers.

Table 10. Average change between the historic and present-day sensitivity simulations and the absolute difference.

Joint Temperature Difference				
Temperature	-2	-1	1	2
Average Change	0.03	-0.01	-0.004	0.005
Absolute Difference	1.03	1.24	0.97	0.89

## CHAPTER 5

### DISCUSSION AND CONCLUSIONS

#### 5.1 Control Simulation Evaluation

After the present-day control simulation was compared to observational data it was found that WRF overestimated the precipitation totals, with a majority of the precipitation falling on a single date instead of being well-distributed like the observational data. This overshoot of precipitation was found across all weather stations tested. Comparing observed precipitation to simulated data can be difficult because of the lack of spatial coverage for the observed data, and any change in the precipitation pattern for the simulation can drastically change the precipitation totals in the areas of interest.

Analysis of the historic and present-day simulations shows very little difference between precipitation values across both domains. Within domain 3, there is a very slight increase in precipitation for the 2016 landcover, and a marginally greater precipitation total for the 1938 landcover within domain 2, which has substantially more non-urban areas compared to the 2016 data set. When analyzing Figure 21, there is no pattern found between the initial simulations' precipitation, although, within the 3<sup>rd</sup> domain, some of the greatest precipitation differences are located near where industrial/commercial landcover was located within the present-day simulation.

The average temperatures over the course of each simulation were calculated and compared to each other to determine how landcover affected the T2 values. Figure 22 shows a clear outline around both the urban core of Kansas City along with the urban sprawl that developed between 1938 and 2016. A clear temperature difference over Leavenworth, Kansas in the north and Lawrence, Kansas to the west can also be observed. The added

precipitation during this simulation helped develop these clear distinctions in urban and non-urban areas. When precipitation falls to the ground it cools releasing the energy as sensible heat flux. The difference in temperature of the surfaces allows the distinction between the urban and non-urban areas because of how fast the different surfaces cool through this process.

## 5.2 Sensitivity Simulation Analysis

Four additional simulations were conducted for both the 2016 and 1938 landcover apart from the initial simulations. The first set to be analyzed was the present-day simulation where an increase and decrease of 1° and 2°C was applied to every layer of the atmospheric temperature to simulate anticipated warming and its effect on a precipitation event. The present-day sensitivities precipitation changed about ~10-12% per 1°C, which followed more closely with the super-C-C scaling that was discussed earlier in the Introduction. In the study done by Allen and Ingram (2002), they found a range of 6.5% closer to the poles while closer to the equator could see as high as 25%. This fits with the findings in this study being in the mid latitudes and falling near the middle for both a decrease and increase in temperatures. In the study done by Lenderink (2011), they found results very close to those of this study near 12 to 14%. It is believed that the cause of this super-C-C scaling is due to latent heat release which could cause a positive feedback loop (Trenberth et al., 2003). In the tropics where precipitation is driven through convection, this latent heat release can cause precipitation increases closer to the super-C-C scaling (Allen and Ingram, 2002, Lenderink, 2011).

When the T2 values were evaluated between both initial simulations and sensitivity simulations the results showed that both historic and present-day had an average temperature

change of approximately 0.60°C change per 1°C increase or decrease. However, when looking at the max temperature difference from the controls, it was the historic 1938 simulations that showed the greatest T2 difference. This difference in max temperature difference could be due to the greater amounts of precipitation that fell in the 1938 sensitivity simulations.

### 5.3 Joint Analysis

As discussed in the previous section the 1938 simulation was shown to have greater precipitation values in almost every sensitivity simulation tested compared to its 2016 counterpart. The only outcomes that showed more precipitation for 2016 were the values for both +/-2°C for domain 3. This increase in precipitation for the historic simulations could be due to the increased moisture in the undeveloped land surrounding the core of Kansas City. The lack of urban development in surrounding areas may have caused a greater amount of water to be stored in the ground, which could be used as kindling for evaporation, allowing more moisture to be present in the atmosphere.

When the analysis was done on the T2 difference between historic and present-day simulations, one can see clear area around the urban sprawl that developed between 1938 and 2016 can be seen. This urban sprawl area has a clear increased temperature for 1938, however in the urban core it is flipped, and that area is cooler in 1938. This warming of the non-urban area for the 1938 simulation could be caused by different cooling rates between rural and urban landcover. This effect would need to be evaluated in a separate study to further understand this relationship. The average change in T2 over domain 3 between

corresponding 1938 and 2016 simulations was found to be very minimal with an absolute difference of close to 1°C between each comparison.

#### 5.4 Conclusion

In recent history we have begun to see more intense precipitation events that have led to devastating flooding across the Midwest. This increase in precipitation, according to the IPCC, is expected to increase, which would cause significant damage to our infrastructure and agriculture in this area. In this study, the increase in precipitation per degree Celsius stayed constant amongst both land cover simulations, with 10-15% increase across all simulations. This increase follows the super-CC scaling found in other studies (Lenderink, 2011, Allen and Ingram, 2002). The change in land cover did not affect the total precipitation value. In the areas that were left unchanged between historic and present-day simulations, near surface air temperatures were found to be warmer in the present-day simulations. The outer urban sprawl that developed between 1938 and 2016 showed cooler temperatures compared to the historic non-urban area. This effect could be attributed to the change in latent heat flux allowing evaporation to cool the surface of the urban areas much quicker than the non-urban areas. While this study did not show a difference between the historic and present-day simulations for precipitation, it did show that we can be expected to see an increase in extreme precipitation at closer to 10-15% per degree Celsius.

A limiting factor of this study is the use of only a single precipitation event. Analysis of additional precipitation events and events during different parts of the year could provide additional information on this topic. However, precipitation is expected to decrease in the

summer and fall months around the Kansas City area, so events should be simulated outside of these seasons.

## REFERENCES

- Abatzoglou, John T., and Timothy J. Brown. “A Comparison of Statistical Downscaling Methods Suited for Wildfire Applications.” *International Journal of Climatology*, vol. 32, no. 5, 2012, pp. 772–80. *Wiley Online Library*, doi:[10.1002/joc.2312](https://doi.org/10.1002/joc.2312).
- Ali, Haider, et al. “Global Observational Evidence of Strong Linkage Between Dew Point Temperature and Precipitation Extremes.” *Geophysical Research Letters*, vol. 45, no. 22, 2018, p. 12,320-12,330. *Wiley Online Library*, doi:[10.1029/2018GL080557](https://doi.org/10.1029/2018GL080557).
- Allen, Myles R., and William J. Ingram. “Constraints on Future Changes in Climate and the Hydrologic Cycle.” *Nature*, vol. 419, no. 6903, Springer Nature, Sept. 2002, p. 224. doi:[10.1038/nature01092](https://doi.org/10.1038/nature01092).
- Barbero, R., et al. “Is the Intensification of Precipitation Extremes with Global Warming Better Detected at Hourly than Daily Resolutions?” *Geophysical Research Letters*, vol. 44, no. 2, 2017, pp. 974–83. *Wiley Online Library*, doi:[10.1002/2016GL071917](https://doi.org/10.1002/2016GL071917).
- Chen, Shien-Tsung, et al. “Statistical Downscaling of Daily Precipitation Using Support Vector Machines and Multivariate Analysis.” *Journal of Hydrology*, vol. 385, no. 1–4, May 2010, pp. 13–22. doi:[10.1016/j.jhydrol.2010.01.021](https://doi.org/10.1016/j.jhydrol.2010.01.021).
- Davenport, Frances V., et al. “Contribution of Historical Precipitation Change to US Flood Damages.” *Proceedings of the National Academy of Sciences*, vol. 118, no. 4, Jan. 2021, p. e2017524118. doi:[10.1073/pnas.2017524118](https://doi.org/10.1073/pnas.2017524118).
- Gall, Melanie, et al. “The Unsustainable Trend of Natural Hazard Losses in the United States.” *Sustainability*, vol. 3, no. 11, pp. 2157–2181, doi:[10.3390/su3112157](https://doi.org/10.3390/su3112157).
- Hou, Yu-kun, et al. “Comparison of Multiple Downscaling Techniques for Climate Change Projections given the Different Climatic Zones in China.” *Theoretical & Applied*

*Climatology*, vol. 138, no. 1/2, Springer Nature, Oct. 2019, pp. 27–45. doi:[10.1007/s00704-019-02794-z](https://doi.org/10.1007/s00704-019-02794-z).

Huffstutter, P. J. “Climate Signals | Exclusive: More than 1 Million Acres of U.S. Cropland Ravaged by Floods.” *Climate Signals*, 29 Mar. 2019, <https://www.climatesignals.org/headlines/exclusive-more-1-million-acres-us-cropland-ravaged-floods>.

IPCC, 2014: Climate Change 2014: Synthesis Report. Contribution of Working Groups I, II and III to the Fifth Assessment Report of the Intergovernmental Panel on Climate Change [Core Writing Team, R.K. Pachauri and L.A. Meyer (eds.)]. IPCC, Geneva, Switzerland, 151 pp.

IPCC, 2018: Global warming of 1.5°C. An IPCC Special Report on the impacts of global warming of 1.5°C above pre-industrial levels and related global greenhouse gas emission pathways, in the context of strengthening the global response to the threat of climate change, sustainable development, and efforts to eradicate poverty [V. Masson-Delmotte, P. Zhai, H. O. Pörtner, D. Roberts, J. Skea, P.R. Shukla, A. Pirani, W. Moufouma-Okia, C. Péan, R. Pidcock, S. Connors, J. B. R. Matthews, Y. Chen, X. Zhou, M. I. Gomis, E. Lonnoy, T. Maycock, M. Tignor, T. Waterfield (eds.)]. In Press.

Iacono, Michael J., et al. “Radiative Forcing by Long-Lived Greenhouse Gases: Calculations with the AER Radiative Transfer Models.” *Journal of Geophysical Research*, vol. 113, no. D13, July 2008, p. D13103. doi:[10.1029/2008JD009944](https://doi.org/10.1029/2008JD009944).

Irfan, Umair. “Extreme Weather Has Again Damaged a Major Military Base.” *Vox*, 25 Mar. 2019, <https://www.vox.com/2019/3/25/18280758/nebraska-flooding-air-force-offutt>.

Janji, Zaviša I. *Nonsingular Implementation of the Mellor-Yamada Level 2.5 Scheme in the NCEP Meso Model*. 2002, p. 61.

- Janji, Zaviša I. “The Step-Mountain Eta Coordinate Model: Further Developments of the Convection, Viscous Sublayer, and Turbulence Closure Schemes.” *Monthly Weather Review*, no. 122, 1994, pp. 927–45, doi:[https://doi.org/10.1175/1520-0493\(1994\)122<0927:TSMECM>2.0.CO;2](https://doi.org/10.1175/1520-0493(1994)122<0927:TSMECM>2.0.CO;2).
- Janji, Zaviša I. “The Surface Layer in the NCEP Eta Model.” *American Meteorological Society*, Aug. 1996, p. 354.
- Kain, John S. “The Kain–Fritsch Convective Parameterization: An Update.” *Journal of Applied Meteorology and Climatology*, vol. 43, no. 1, American Meteorological Society, Jan. 2004, pp. 170–81. [journals.ametsoc.org](https://journals.ametsoc.org), doi:[10.1175/1520-0450\(2004\)043<0170:TKCPAU>2.0.CO;2](https://doi.org/10.1175/1520-0450(2004)043<0170:TKCPAU>2.0.CO;2).
- Le Roux, Renan, et al. “Comparison of Statistical and Dynamical Downscaling Results from the WRF Model.” *Environmental Modelling & Software*, vol. 100, Feb. 2018, pp. 67–73. doi:[10.1016/j.envsoft.2017.11.002](https://doi.org/10.1016/j.envsoft.2017.11.002).
- Lenderink, G., et al. “Super-Clausius–Clapeyron Scaling of Extreme Hourly Convective Precipitation and Its Relation to Large-Scale Atmospheric Conditions.” *Journal of Climate*, vol. 30, no. 15, American Meteorological Society, Aug. 2017, pp. 6037–52. [journals.ametsoc.org](https://journals.ametsoc.org), doi:[10.1175/JCLI-D-16-0808.1](https://doi.org/10.1175/JCLI-D-16-0808.1).
- Mesinger, F., et al. *North American Regional Reanalysis: Evaluation Highlights and Early Usage*. May 2005, pp. A21B-06.
- Monin, A. S., and A. M. Obukhov. *Basic Laws of Turbulent Mixing in the Surface Layer of the Atmosphere*. 1954, p. 30.
- Nakanishi, Mikio, and Hiroshi Niino. “An Improved Mellor–Yamada Level-3 Model: Its Numerical Stability and Application to a Regional Prediction of Advection Fog.” *Boundary-*

*Layer Meteorology*, vol. 119, no. 2, May 2006, pp. 397–407. doi:[10.1007/s10546-005-9030-8](https://doi.org/10.1007/s10546-005-9030-8).

Nakanishi, Mikio, and Hiroshi Niino. “Development of an Improved Turbulence Closure Model for the Atmospheric Boundary Layer.” *Journal of the Meteorological Society of Japan. Ser. II*, vol. 87, no. 5, 2009, pp. 895–912. doi:[10.2151/jmsj.87.895](https://doi.org/10.2151/jmsj.87.895).

NASA. *Midwest Flooding March 2019 | NASA Applied Sciences*. 18 Mar. 2019, <http://appliedsciences.nasa.gov/what-we-do/disasters/disasters-activations/midwest-flooding-march-2019>.

National Oceanic and Atmospheric Administration. *What Is Bombogenesis?* 26 Feb. 2021, <https://oceanservice.noaa.gov/facts/bombogenesis.html>.

Nebraska Department of Natural Resources. “Nebraska Flooding: March 2019.” *ArcGIS StoryMaps*, 19 Dec. 2019, <https://storymaps.arcgis.com/stories/9ce70c78f5a44813a326d20035cab95a>.

Norvell, Kim. “Number of Levee Breaches up to 30 from 12, and Iowa’s Flood Season Is Just Getting Started.” *Des Moines Register*, 20 Mar. 2019, <https://www.desmoinesregister.com/story/news/2019/03/20/iowa-flooding-2019-weather-rain-snowmelt-levees-breached-flood-warnings-where-forecast-southwest-nws/3224920002/>.

Olson, Joseph B., et al. *A Description of the MYNN-EDMF Scheme and the Coupling to Other Components in WRF–ARW*. Earth System Research Laboratory (U.S.), Global Systems Division, 2019. doi:[10.25923/N9WM-BE49](https://doi.org/10.25923/N9WM-BE49).

Pierce, David W., et al. “Improved Bias Correction Techniques for Hydrological Simulations of Climate Change.” *Journal of Hydrometeorology*, vol. 16, no. 6, American Meteorological Society, Dec. 2015, pp. 2421–42. *journals.ametsoc.org*, doi:[10.1175/JHM-D-14-0236.1](https://doi.org/10.1175/JHM-D-14-0236.1).

Rachelle Blake. *Team Offutt Battling Flood Waters*. 17 Mar. 2019,

<https://www.offutt.af.mil/News/Photos/igphoto/2002102304/>.

Skamarock, W. C., Klemp, J. B., Dudhia, J., Gill, D. O., Barker, D., Duda, M. G., ... Powers, J. G.

(2008). *A Description of the Advanced Research WRF Version 3* (No. NCAR/TN-475+STR).

University Corporation for Atmospheric Research. doi:10.5065/D68S4MVH

Sohl, Terry L., et al. "Modeled Historical Land Use and Land Cover for the Conterminous United

States." *Journal of Land Use Science*, vol. 11, no. 4, 2016, pp. 476–99,

doi:[10.1080/1747423X.2016.1147619](https://doi.org/10.1080/1747423X.2016.1147619). USGS Publications Warehouse.

Stock, Charles. *Climate Model Downscaling*. [https://www.gfdl.noaa.gov/climate-model-](https://www.gfdl.noaa.gov/climate-model-downscaling/)

[downscaling/](https://www.gfdl.noaa.gov/climate-model-downscaling/). NOAA.

Tandon, Neil F., et al. "Understanding the Dynamics of Future Changes in Extreme Precipitation

Intensity." *Geophysical Research Letters*, vol. 45, no. 6, 2018, pp. 2870–78. *Wiley Online*

*Library*, doi:[10.1002/2017GL076361](https://doi.org/10.1002/2017GL076361).

Tewari, M., et al. *14.2A Implementation And Verification Of The Unified Noah Land Surface*

*Model In The WRF Model*. 2004, p. 6.

Thompson, Gregory, et al. "Explicit Forecasts of Winter Precipitation Using an Improved Bulk

Microphysics Scheme. Part II: Implementation of a New Snow Parameterization." *Monthly*

*Weather Review*, vol. 136, no. 12, Dec. 2008, pp. 5095–115. doi:[10.1175/2008MWR2387.1](https://doi.org/10.1175/2008MWR2387.1).

Trenberth, Kevin E., et al. "The Changing Character of Precipitation." *Bulletin of the American*

*Meteorological Society*, vol. 84, no. 9, American Meteorological Society, Sept. 2003, pp.

1205–18. [journals.ametsoc.org](https://journals.ametsoc.org), doi:[10.1175/BAMS-84-9-1205](https://doi.org/10.1175/BAMS-84-9-1205).

United States Army Corps of Engineers. *2021 Report Card for America's Infrastructure*. Mar. 2021, pp. 47–51, [https://infrastructurereportcard.org/wp-content/uploads/2020/12/National\\_IRC\\_2021-report.pdf](https://infrastructurereportcard.org/wp-content/uploads/2020/12/National_IRC_2021-report.pdf).

US Department of Commerce, NOAA. *Monthly Climate and Records*. NOAA's National Weather Service, 19 Dec. 2019, [https://www.weather.gov/oax/monthly\\_climate\\_records](https://www.weather.gov/oax/monthly_climate_records).

van Vuuren, Detlef P., et al. "The Representative Concentration Pathways: An Overview." *Climatic Change*, vol. 109, no. 1–2, Nov. 2011, pp. 5–31. doi:[10.1007/s10584-011-0148-z](https://doi.org/10.1007/s10584-011-0148-z).

van Vuuren, Detlef P., and Keywan Riahi. "The Relationship between Short-Term Emissions and Long-Term Concentration Targets: A Letter." *Climatic Change*, vol. 104, no. 3–4, Feb. 2011, pp. 793–801. doi:[10.1007/s10584-010-0004-6](https://doi.org/10.1007/s10584-010-0004-6).

Van Uytven, Els, et al. "Uncovering the Shortcomings of a Weather Typing Method." *Hydrology & Earth System Sciences*, vol. 24, no. 5, Copernicus Gesellschaft mbH, May 2020, pp. 2671–86. doi:[10.5194/hess-24-2671-2020](https://doi.org/10.5194/hess-24-2671-2020).

"Winter Storm Ulmer, the March 2019 Bomb Cyclone, Blasted the Plains With Blizzard Conditions, High Winds | The Weather Channel - Articles from The Weather Channel | Weather.Com." *The Weather Channel*, 15 Mar. 2019, <https://weather.com/storms/winter/news/2019-03-11-winter-storm-ulmer-forecast-west-plains-blizzard-conditions>.

Xu, Zhongfeng, et al. "Dynamical Downscaling of Regional Climate: A Review of Methods and Limitations." *Science China Earth Sciences*, vol. 62, no. 2, Feb. 2019, pp. 365–75. doi:[10.1007/s11430-018-9261-5](https://doi.org/10.1007/s11430-018-9261-5).

## VITA

Kevin Kandola graduated from the University of Missouri – Kansas City where he received Magna Cum Laude for his Bachelor of Science in Geography with an undergraduate certificate in GIS in May 2019. He then returned the following semester to complete his Master of Science in Earth and Environmental Science. While at UMKC he worked with Dr. Fengpeng Sun as an undergraduate and graduate research associate.

In January 2019, Kevin was able to attend a week-long workshop for the use of Weather Research and Forecasting (WRF) model at the National Center for Atmospheric Research in Boulder, Colorado. Kevin has been able to present his work at the SUROP symposium in the December 2019, the 2020 AGU Fall meeting and the 2020 AMS meeting both of which were done virtually.